Response to referee comments

[Seismic monitoring of small alpine rockfalls validity, precision and limitations]
July 13, 2017

We would like to thank the referee for the encouraging and helpful comments, all of them obviously devoted to improve the quality and impact of the manuscript.

Referee 2.1: *Title: When first reading the title of the paper I was expecting an analysis of the feasibility to study rockfalls with seismic methods in different contexts, or an enriched review of past studies on this subject. "Validity" and "limitations" of seismic rockfalls monitoring in general are not discussed in this paper and I find that what the authors propose is essentially an interesting case study. This should be explicit and clarified in the title. I would suggest for example: "Validity, precision and limitations of the seismic detection and location of small rockfalls in the Swiss Alps".*

Reply: We understand the arguments and changed the title (almost) as suggested.

Referee 2.2: *P2 L17: Please order the references chronologically. There is a wealth of studies on landslides seismic signals. If you decide to select some of them as examples, use "e.g." before citing them.*

Reply: All reference lists were checked for chronological order and corrected where necessary. The term "e.g." was inserted as suggested.

Referee 2.3: *P2 L18: While it would be an honor to share the name of David Hilbert, I am not. Here and everywhere else please correct the references to "Hibert et al." (no "L").*

Reply: Indeed, this was an unecessary bug that sneeked into the tex file. It has been corrected throughout.

Referee 2.4: *P2 L21: "cf" not necessary here or elsewhere.*

Reply: Terms have been removed where necessary/appropriate.

Referee 2.5: *P3 L14: Is this different from spectrograms?*

Reply: The term has been replaced by "spectrograms".

Referee 2.6: *P3 L19: Burtin et al. [2016] were not the first to show that seismic signals generated by rockfalls are dominated by surface waves. In the references here you can add Deparis et al., [2008], Dammeier et al., [2011], and Levy et al., [2015].*

Reply: References included as suggested.

Referee 2.7: *P3 L22: "Vital" seems a bit strong. Interesting? Significant? Crucial?*

Reply: Changed to "unique, important". We believe that this is the best phrase to describe the value of seismic data with respect to the level of detail they can provide in some cases, e.g., as shown in the example figure 2.

Referee 2.8: *Section 3: Is this section necessary? Could you move this into the introduction?*

Reply: We had thought about adding this chapter to the introduction during the writing process but then decided to keep it separate, mainly to adequately set the scope for the entire manuscript: i) "We know that seismic monitoring works for characterising rockfall, but there is a set of unknowns at the moment" and ii) "For those who are unfamiliar with the seismic approach, this is what the data looks like one can record and has to interpret". Furthermore, this section already presents results of this study, which makes it difficult to include it to the introduction. Thus, we prefer to keep the section in its current form, also backed up by no such impression by any of the three other referees.

Referee 2.9: *P3 L28: What is the "limit of detection"? Is it the targeted (or the possible?) resolution of the point clouds?*

Reply: This term is common jargon among the TLS community. We added a short definition in brackets for comprehension by a wider readership.

Referee 2.10: *P4 L3: Are the seismometers 3 components? Please add this information here. Figure 2 – caption: Do you know the volume of this* *particular event? If so this information could be added in the caption. Are the signals filtered?*

Reply: Component information was added as suggested. Released rock volume, event ID and link to table 1 are provided in the caption, now. Filter window (1–90 Hz) is given in the caption, as well.

Referee 2.11: *P6 L17: The STA-LTA ratio picker was first proposed by Allen [1982].*

Reply: Reference was changed as suggested.

Referee 2.12: *P6 L18: Envelopes of seismic signals are commonly computed from the Hilbert transform of the signal. I think using the absolute amplitude is not a problem for detection, but for a localisation method based on the cross-correlation of envelopes,the Hilbert transform might yield better results. While I certainly do not think it is necessary to redo the current analysis with Hilbert envelopes, I would suggest testing this in future studies.*

Reply: Absolutely correct. The utilised algorithm used the Hilbert (with l this time) transform to calculate the envelope. The main idea in the original manuscript was to provide the unfamiliar reader with a short explanation of the term "envelope". However, obviously this plan was misleading. We removed the short and wrong definition, now.

Referee 2.13: *P6 L24: Can you indicate here what are the threshold values chosen?*

Reply: Since these values are part of the results, we provide here now the link to the adequate chapter (5.2), where these values are presented and justified.

Referee 2.14: *P7 L1 and 11: You choose here a velocity for S-waves but as stated before rockfalls seismic signals are dominated by surfaces waves (which are slower than body waves). How many events have you excluded based on this criterion?*

Reply: We have added further credit to earlier studies that point at the value of 2000 m/s for land slides and rock falls. Actually, after a test re-run of the approach on a short section of the data base with lower velocities, all additionally included events were rain drop impacts (based on the short duration of the picks and relation to the meteorolgical data).

Referee 2.15*: P7 L10-11: This is a bit confusing. You first had an automated exclusion criterion based on the time delay between the onsets of the waves recorded at each station of the network and then you still check manually if this criterion is verified? What is the point of the first automated exclusion then? Maybe reorganize this paragraph and the one just before to improve clarity.*

Reply: Indeed, point i) and ii) are redundant. The initial idea was to have all decision/rejection criteria at one place as a summary. However, this was confusing. We removed these two points.

Referee 2.16*: P7 L13-14: Criterion iv): Does this imply that you know the location of the events before manually selecting the signals?*

Reply: The section was rephrased to be more general, it now simply expresses that the signals are expected to show a significant difference in their amplitudes due to the different source–receiver distances causing attenuation. If the source is inside the network, the differences between source and receiver for all possible station pairs is expected to be much higher than for a source location outside the network, especially if the source is away several times the network aperture, when only site amplification effects may modify the picture.

Referee 2.17*: P7 L17: References : "e.g." or add at least Surinach et al. [2005].*

Reply: Both suggestions were implemented.

Referee 2.18*: P7 L20: "Multiptaper" Typo?*

Reply: Yes, the typo has been corrected.

Referee 2.19*: P7 L21: References : "e.g.". Hibert et al. [2011] and Dammeier et al. [2011] seem more appropriate references here.*

Reply: Included/corrected as suggested.

Referee 2.20*: P7 L29-34: The approach proposed by Hibert et al. [2014 and not 2011] is designed to overcome all the issues regarding the specificity of rockfall seismic signals you enumerate before this sentence (emergent onset, waveform discrepancies, absence of seismic phases, high-frequency). Moreover if the dominant issue is the "differences between waveform properties at different stations" the cross-correlation approach would not work. In your case you can use a method based on the cross-correlation of the signal waveforms because the signals recorded at different stations are not too dissimilar. I suspect this is the case because the aperture of your network is not large (inter-station distances of 1 km). This is not the case at the Piton de la Fournaise volcano and is one of the difficulties that forced us to develop a new kurtosis-based first-arrival picker that is accurate enough to pick emergent signals. Please rewrite this paragraph by taking this remark into account.*

Reply: As suggested, the paragraph has been rewritten.

Referee 2.21*: P8 L19-21: Topography correction is necessary because rockfalls generate surface waves that propagate following the topography. Also the correct reference is Hibert et al. [2014] and not [2011] here.*

Reply: The text was changed as suggested and the reference was corrected.

Referee 2.22*: P8 L8-18: If you change the frequency range used to find the time lag that yields the best cross-correlations this should have an impact on the optimal velocity, and vice versa. Can you elaborate on the interdependence of the optimal frequency bands and the optimal velocities found? It can be interesting to add in Table 2 the velocity that gives the best location for these 10 rockfalls.*

Reply: As suggested, this section does now discuss the interconnectivity of wave velocity and frequency range used in the location routine. Since we kept the wave velocity constant for the different frequency bands there is limited value in adding it to the data table.

Referee 2.23*: P8 L21-22: Not all Earth surface processes generate seismic signal dominated by surface waves. I suggest to change "other Earth surface processes" into "other mass movement processes" or "gravitational processes". Also see comment on P3 L19 regarding the reference to Burtin et al., [2016].*

Reply: Changed as suggested.

Referee 2.24: *P8 L22-25: It is not clear how you performed this correction. What is: "that part where direct distance is above the actual surface elevation"? Does this mean that you corrected the direct straight line distance from pixel to pixel by the slope angle? Did you compute profiles for each pixel-station pair from the intersection of the straight line between those two points with the grid points of your DEM? Integrating the topography in propagation maps is not a trivial task but as you mentioned is critical to have accurate locations of rockfalls. This should be a bit more detailed, especially if the main focus of this paper is the capability to locate rockfalls from the seismic signal they generate.*

Reply: We added further explaining sentences. The approach is a direct translation of the Matlab based technique discussed by Burtin et al. (2014, ESurf) to the language R and is part of the freely available package eseis.

Referee 2.25: *P8 L30: Please define what is the "likelihood quantile" before.*

Reply: This value is now defined at this position and used throughout the text. P is the location cross-correlation value of a given pixel and the 0.95 quantile is the threshold value arising from all P values of the location grid used to, e.g., clip the location polygons.

Referee 2.26: *P9 L26: What caused this tilting? Do you know when it started? What is the influence of this tilting on the seismic signals recorded before dismantling those stations?*

Reply: The (most likely) cause of the tilting is now mentioned in the text. It is hard to say when this started because the TC120s sensors can compensate tilting up to about 10 degrees by using additional battery power but suddenly fail to record further data once beyond this tilting angle. Anyhow, we think this technical detail about the utilised sensor is of limited use for the reader and prefer not to infuse it into the text.

Referee 2.27: *P11 L16-18: I am a bit sceptical regarding the "rain drop sources" because you have buried your stations at 30-40 cm depth. This should prevent any direct contact between the seismometers and rain drops and I think rain drops are too weak seismic source to generate signals that would not be attenuated in the first few centimeters of propagation. Other common sources that can generate impulsive signals with energy in high-frequency bands are thunder, numerical glitches or close footsteps (animal or human). You based your attribution of those signal to rain drops from* *the observation that "it only occurs in the records when it was raining in the Lauterbrunnen Valley during deployment and maintenance of stations". So you observe these noise signals on the days you were on the sites. There is a possibility that these signals are your footsteps, but without clear evidences we do not know. So did you observed those signals on days where you were not on site? Can you provide other arguments to attribute those signals to rain drops? For example, did you observe that those signals appeared and disappeared gradually over a period of times of several tens of minutes (or few hours), mimicking the passing of scattered showers? If so could you show this on a figure to definitely convince your readers that those signals are indeed generated by rain drops? If not I would suggest to rename this class of source to "impulsive noise".*

Reply: We added a further figure showing the co-occurrence of the seismic signal pulses and a rain data record. The data is also interpreted in the text and we argue for the rain cause with respect to passing animals or humans on the base of the irrgularity of the signals.

Referee 2.28: *P14 L3-4: What is "n"? What is "r"?*

Reply: "n = 8" has been replaced by "eight cases" and "r" has been removed completely, see comments of referee three.

Referee 2.29: *P14 L4: If you want to provide to the readers an analysis based on the SNR you need to indicate how you have computed this quantity before.*

Reply: The term SNR is now defined where it is used for the first time (chapter 4.3).

Referee 2.30: *P17 L13-14: What are those relationships? Do you refer to the studies of Hibert et al. [2014], Manconi et al. [2016]? Dammeier et al. [2016]?*

Reply: The statement is now supported by some of the suggested references.

Referee 2.31: *P17 L20-21: Levy et al. [2015] used a different approach (first-arrival picking and not cross-correlation back propagation as in the present study) and had a network with a much larger aperture (inter-stations distances of few kilometers).*

Reply: Corrected as suggested.

Referee 2.32: *P18 L7-9: I agree with the assumption that a rockfall with a higher volume should generate a higher-amplitude seismic signal if the travelled path and the fall height are the same. However you say latter that in your case there are no correlation between seismic energy/amplitude and the volumes of the events.*

Reply: We rewrote the statement further down to say explicitly that it refers to relationships based on volume, only. In the Lauterbrunnen Valley case we would have to include many more parameters than just rock volume, as explained in the rest of this paragraph. So in summary, both parts are true: in the case where only the rock volume is different while all other parameters (e.g., height, fragmentation, debris entrainment and impact location) are identical, the seismic signal of a larger rock mass will undoubtly be larger. But when all the other parameters can vary, as well, this energy-volume relationship will fade.

Referee 2.33: *P18 L12-13: The volume of the rockfalls in the study by Hibert et al. [2011] had volumes as low as few cubic meters.*

Reply: The sentence was rephrased and more appropriate references were used, now.

Referee 2.34: *P18 L18-19: Indeed, you are working with complicated events and I acknowledge that extracting quantitative laws might be difficult in this case. However, as shown by the example discussed in section 6.3, you are able to identify the different stages of the rockfall propagation. Is this true for the 10 rockfalls in your database? If so, you have every information you need (location of the events, volumes/masses, average velocity of the medium) to go further in your analysis. For example, what are the relationships between the first impulsive arrival amplitude (corrected from propagation effect) (phase 1) and the volume? The relationships between the seismic energy and the potential energy lost at the first impact with the topography (phase 2) ? The same relationships during the propagation phase on the talus (phase 3)? Those are fundamental issues that you might be able to contribute to answer with your dataset. Even if no relationships are found, this would still be very interesting as it will nourish discussion on the validity for small rockfalls of the relationships found by others [e.g. Deparis et al., 2008; Vilajosana et al., 2008; Hibert et al., 2011; Dammeier et al., 2011; Yamada et al., 2012; Ekström and Stark, 2013; Farin et al., 2015; Levy et al., 2015; Hibert et al., E-Surf in press]. I understand that this might be out of the scope of this study, but I think that adding this deeper analysis will significantly improve the impact and the reach of your paper.*

Reply: Indeed, for some of the events there is a comparably favourable situation as for the event shown in figure 2, but this would reduce the number of suitable cases to about four. We believe this is not a sufficient amount of data to hypothesise about quantitative laws. As suggested by the referee, the topic is out of the manuscript scope and extending the discussion to this theme would inevitably require a significant redesigning process of the entire mansucript, a point we consider not balanced by the number of suitable events that can be used to support claims in the light of this goal. We have however opened the door for the reader to think about this possibility at the end of the paragraph (last two sentences).

Referee 2.35: *P18 L31: references : add "e.g." and/or other references, for example : Helmstetter and Garambois [2010], Yamada et al., [2012], Zimmer and Sitar., [2015], Hibert et al. [2017].*

Reply: Both suggestions were included.

Referee 2.36: *P19 L3-5: While it seems reasonable to think that large mass detachments are preceded by cracking and fracture opening that generates an increasing rate of micro-earthquakes, this is more debatable for very small rockfalls such as the ones in this study. Another assumption to explain this first impulsive signal is that it is generated by the rebound of the Earth in the departure zone due to the detachment of the mass. This was observed at Piton de la Fournaise volcano [Hibert et al., 2011]. I think both assumptions should be mentioned here.*

Reply: Implemented as suggested.

Referee 2.37: *P19 16-17: If larger particles have higher momentum they will reach the bottom of the slope more rapidly than small particles. In fact this is what is observed in many cases on video recordings of events: large blocks preceding the flow of small granular materials. The loss of high-frequency at the end of seismic signals generated by gravitational instabilities is complex and still not yet fully understood. Analytical models [e.g. Okal, 1990; Farin et al., 2015] suggest that events with larger volume will indeed generate signal with a lower corner frequency, but the overall amplitude of the signal across the whole frequency range will be higher. To this adds the fact that high frequencies generated by small particles are more attenuated. The combination of those two processes suggests that the loss of high-frequency at the end of those seismic signals is due to the early immobilization of the largest particles, not the smallest. This is highly speculative, and any* *interpretation of this frequency shift has to be done carefully and supported by data. If you want to comment on this, please add references.*

Reply: As this part of the anatomy section is not a central part of the scope of the manuscript we followed the referee suggestion. We removed the speculative part and provide a reference to support the first part.

Response to referee comments

[Seismic monitoring of small alpine rockfalls validity, precision and limitations]
July 13, 2017

We would like to thank the referee for the encouraging and helpful comments, all of them obviously devoted to improve the quality and impact of the manuscript.

Referee 3.1: *This manuscript presents a new approach for detecting and locating rockfalls using seismic signals, applied to a case study in the Swiss Alps. I find the manuscript well written, well organized and the results interesting. Validity and precision of the method have been carefully discussed, while I found the discussion about possible limitations a bit dry. I suggest to improve this part, especially given the fact that several manual adjustments and optimizations are needed in post-processing. Below are some minor comments about the main text and the supplementary materials. Specific comments on the main text.*

Reply: We reorganised the discussion and especially the conclusion chapter to highlight the limitation of the seismic method. Also, the need for manual supervision has been added to the abstract, introduction and discussion chapter 6.1 (also see referee comment 17).

Referee 3.2: *Title: I find the title too vague. The title should reflect that the manuscript is about one possible method for seismic rockfall monitoring, applied to a specific case study.*

Reply: As suggested, also by referee 2, the title has been focused with respect to location and event size.

Referee 3.3: *P. 3, Lines 19-20: this would be true if seismic waves were travelling in a homogeneous medium. When looking at high frequencies, like in this study, seismic waves are mostly sensitive to the crust and therefore their travel time is strongly affected by crustal heterogeneities and shallow slow velocity layers. Seismic tomographies of the Alps have shown crustal heterogeneities as large as 20.*

Reply: The additional information is now included, making lcear that the homogeneous medium is an idealised case and that under natural conditions there can be significant alterations.

Referee 3.4: *Figure 1: a large-scale map, showing the Lauterbrunnen Valley on a larger context, would be informative.*

Reply: Overview map of Switzerland and the location of the study area therein has been added.

Referee 3.5: *Figure 2 and 4: the power spectral density is usually normalized to the frequency bin width and therefore the unit is (m/s)/Hz. Why this is not the case here?*

Reply: The missing legend item has been added.

Referee 3.6: *P. 6, Line 23: how the length of the STA and LTA windows affects your results? How these two values have been chosen?*

Reply: Indeed, the window length obviously affect the number and timing of initially picked events. We added an explaining sentence for clarification. Our reasoning for chosing these values is and was based on the referenced study of Burtin et al. (2014), as stated in the manuscript. It is hard to inspect how different values of STA and LTA window lengths would affect the results because the picking is just the start of a long chain of further steps to remove spurious events. We think adding information of other window lengths would add little further information to trace the overall contribution to the final number of events.

Referee 3.7: *P. 6, Line 28: the authors set the minimum cut-off frequency of the filter to 10 Hz, but in Table 1 they also showed that, after adjusting by hand the frequency range for location, 5 rockfalls over 10 are detected at minimum frequencies lower than 10 Hz. Please discuss this point.*

Reply: Indeed, the filter frequency window for location is different than for picking. For picking, the main goal is to have it matching most of the envisioned events and not to already focus on the actual frequency content of the individual rockfalls. We believe that this point is clear by referring to the four studies that noted the typical frequency content of rockfalls. The referee is absolutely correct that the filter frequencies to optimise the location estimate are lower than 10 Hz for many events. We comment on this point now in section 6.1.

Referee 3.8: *P. 7, Lines 13-14: criterion (iv) is basically the geometrical spreading, which is also characteristic of seismic waves generated by earthquakes.*

Reply: The criterion (now cirterion ii) has been clarified to point at the difference of a source inside the network versus a source far away from the network.

Referee 3.9: *P. 7, Line 19: "windows of 1.4 and 1.1 s" are referred to what?*

Reply: The term "moving time windows of 1.4 and 1.1 s to generate the spectra" has been added for clarification.

Referee 3.10: *P. 8, Line 4: "700 to 4000 m/s" is referred to which seismic phase?*

Reply: The term has been replaced by "apparent velocities" and essential references to support it, see comments of referee 2.

Referee 3.11: *P. 10, Lines 2-3: how do you choose the STA/LTA threshold?*

Reply: The values were not chosen from best guesses but are based on the measured waveforms of the control events. The link to this sentence before the statement is now strengthened by linking these two sentences.

Referee 3.12: *Table 2: the default frequency range varies from rockfall to rockfall. How it has been chosen?*

Reply: Please see the justifications in section 4.4, third paragraph.

Referee 3.13: *P. 14, Line 4: The signal-to-noise ratio is strongly related to the amplitude of ambient seismic noise, which may vary in time and space. I think it's difficult to find a correlation with the duration of the event (and in fact, the correlation coefficient r is pretty small). Please discuss this point.*

Reply: We removed the discussion of the SNR relationships, since – as the referee points out – it is difficult to find these relationships. Furthermore, the information is far from being essential for the scope of the article.

Referee 3.14*: P. 14, Line 9: is 2700 m/s the velocity of S waves? Please, specify the seismic phase associated with the velocity here and everywhere in the paper.*

Reply: As also pointed out by reviewer 2, we clarified the term to "apparent velocity" throughout the manuscript and give adequate references to underline that for such signals it is often not possible to identify the different phases.

Referee 3.15*: P. 16, Line 9 and P.17, Line 28: please, define the threshold value using 3 digits or use the exponential notation.*

Reply: As suggested, we rounded to three digits.

Referee 3.16*: P. 17, Lines 14-16: it seems that, although the algorithm should work automatically, a lot of small manual adjustments are needed in order to get a precise location of the rockfalls. I encourage the authors to discuss more in detail this point, and not just in three lines. Manual adjustments imply a certain level of subjectivity and, in order to ensure reproducibility of the results, this limitation should be discussed carefully.*

Reply: In fact the described workflow is not intended to result in a recipe for automatic rockfall detection and location, especially not for such small events as faced in this study. We added a clarifying sentence about this scope now at the beginning of section 6.1 and also at the end of the introduction and the abstract.

Referee 3.17*: P. 18-19, section 6.3: a recent paper (Gualtieri and Ekstrom, 2017) discussed a similar rockfall behavior. Please discuss your findings in relation with this reference. In particular, they describe the first stage of a rockfall as related to the elastic rebound of the Earth following the mass detachment rather than to the opening and propagating of fracturing. Figure 2 also shows a strong signal at 9:03:48, potentially related to a fourth stage.*

Reply: The article by Gualtieri and Ekstrom (2017) focuses on an event about 10^4 m^3, which is very different from the rockfalls our study focuses on, mainly below 10^0 m^3. The potential source of the signal due to the elastic rebound of the cliff after detachment is now discussed in chapter 6.3, cf. comments of referee 2.

Referee 3.18*: P. 20, Line 17: sensu strictu should be sensu stricto.*

Reply: The term has been corrected.

Referee 3.19: *I have tested the code and I have two main remarks: 1) the pdf with the detailed explanation of the code is very useful, but it would be also good to have the actual code (a file .R) in the folder. 2) The code worked as promised, except for the installation of the package eseis. I had to download and install the package manually. I am working on a Mac OS v. 10.12.4 and I am using Rstudio v. 1.0.136.*

Reply: We are thankful for the invested time to reproduce the results of the study using the same software we used. Initially we considered adding also the set of R scripts to the supplementary materials. However, each fo the about 8 scripts contains hundreds of code lines and would require significant manual adjustments of paths and are actually optimised to automatically create the figures of the manuscript. Thus, they are not optimised for comprehension but for performance.

The installation issue is know to the main author, and related to both the Mac OSX and the current way to host the package on the website. It is intended to release the package on the Comprehensive R Archive Network (CRAN), which will fix the problem. Meanwhile, additional information about installing the package manually is provided on the website of the first author (`http://www.micha-dietze.de/pages/eseis.html`).

Response to referee comments

[Seismic monitoring of small alpine rockfalls validity, precision and limitations]
July 13, 2017

We would like to thank the referee for the encouraging and helpful comments, all of them obviously devoted to improve the quality and impact of the manuscript.

Referee 4.1: *This manuscript applies two methods for studying rockfall activity in the Lauterbrunnen valley. Coupling seismic monitoring and terrestrial laser scanning (TLS) allows a good resolution in time and space, and allows the detection of very small rockfalls. TLS data is used to validate the seismic detection and location method. While seismic monitoring and TLS have been frequently used, coupling both methods is innovative and interesting. The authors obtain impressive results in terms of location accuracy and sensitivity. For these reasons this manuscript is very worth publishing in ESDD. But some changes should be made to clarify a few points.*

Reply: We are thankful for the encouraging feedback and refer to the changes as suggested by the points below.

Referee 4.2: *p6-7. Events detected at different stations are considered to be the same event if the time delay between stations is less than 1.75 s corresponding to an S wave with a velocity of 2000 m/s. I suggest increasing this value to about 10 s, because it is likely that some stations may detect the detachment phase, while other stations may only be triggered by the impact at the cliff base. Another possibility is to merge events at different stations if there is some overlap in time between the signals.*

Reply: In an earlier stage of the project we pursued this concept. However, location of the rockfall events in this study is only possible when the same seismic source (e.g., detachment process or impact) is recorded by all (at least four) stations. Allowing for larger time windows would indeed cause triggering of different event phases by different stations and thus, at best, a smearing of the location estimate. Thus, we need to keep this narrow time window. We explain this necessity now in the STA/LTA paragraph of the revised manuscript.

Referee 4.3: *p13: Events longer than 20 s are removed because this is longer than the expected rockfall propagation. But rockfalls frequently occur in sequences of events, so that this constrain may remove true rockfall events. Here are a few ideas to distinguish automatically earthquakes and rockfalls: Did you use earthquake catalogs to remove earthquakes? The variability of amplitude among stations should be higher for rockfalls (or other nearby sources) than for earthquakes. The time delay between stations should be smaller for earthquakes and other distant sources (deep source implying a higher apparent velocity).*

Reply: Correct, rockfalls – also some of the events described in this manuscript – consist of sequences of activity, including talus slope mobilisation (e.g., event 8). However, the constraint of 20 s is only used for the STA/LTA picker phase. Sequences of releases would result in several subsequent but short STA/LTA picks, as shown in figure 4b of the manuscript. The earthquake catalogues certainly contain the large events during the instrumented period. But smaller, still not rockfall-related events might not be contained in them. We initially tested the variance of signal amplitudes among the stations as a discriminator for earthquakes versus rockfalls but found that the power of this criteria is not high. Indeed, the time delay between stations is usually smaller for earth quakes than for rockfalls. But the duration criterion performed very well in our case, as shown by the average values in the discussed in the text. These points are now mentioned or discussed in the manuscript (chapter 4.3).

Referee 4.4: *P7, l30. You should also cite here Lacroix and Helmstetter (2011) who used a very similar method to locate rockfalls (using the seismic waveforms rather than the signal envelope)*

Reply: Included as suggested.

Referee 4.5: *p8, l30. I do not understand "Locations with a likelihood quantile below 0.95 ..."? Do you mean that you select grid points with cross-correlation smaller than the 0.95 quantile of the distribution of the cross-correlation across the search area? Or do you have a method to estimate the actual probability of a point to be the source location, e.g., as done by Lomax for the nonlinloc location algorithm?*

Reply: We mean the quantile concept. This is now expressed clearly in the manuscript, chapter 4.4, paragraph 5. As suggested by referee 2, the entire section has been revised to clarify this and other points related to better explain the location approach.

Referee 4.6: *I don't see the interest of adjusting the frequency range individually for each event. Of course, it makes the location error smaller. By adjusting more parameters (time interval ...) you could probably lower the location error event more... But what do we learn from that? Adjusting the velocity using all events makes sense, but adjusting one parameter for each event individually does not. Even without optimizing the parameters based on known event location, the location accuracy is quite good considering the number of stations (between 4 and 6)!*

Reply: The main point we want to work out with this exercise is to explore the highest possible location precision available with the data, methodology and landscape setting in this study. Tweaking any other parameters did actually not help improving the location estimate. Obviously, there will never be the chance to go beyond the "unimproved" location frequency approach. We mention this clarification now in the location chapter.

Referee 4.7: *Did you test your location method on synthetic signals? For instance, you can take a real rockfall signal, and shift this signal in time by the difference in travel time to define the signal at the other stations, and add seismic noise. This would provide an optimistic estimate of the location accuracy, because real signals are quite different from one station to another one. It can be useful to estimate the influence of errors on seismic wave velocity.*

Reply: Although such a test with synthetic data would shed more light onto the algorithm performance and capabilities, this manuscript rather follows the natural scale experiment setup. The location approach itself has been discussed in previous studies (cf. Burtin et al., 2013, 2016) and the R-version is a mere translation of it from the Matlab script by Arnaud Burtin and has been validated against this script before releasing the package. See also comment by referee 2.

Referee 4.8: *p17,l24 : The station spacing in your study is quite different from the study of Lacroix and Helmstetter (2011). This study used antennas of 7–24 sensors, with distance between sensors inside an antenna of 20–50 m, and distances between antennas of several hundred meters. Using shorter inter-sensor distance allows correlating the rockfall waveforms rather than their envelope and provides a better location accuracy.*

Reply: The unsuitable reference has been removed to correct the context of the sentence.

Referee 4.9: *p8l5. TLS locations are used to constrain the seismic wave velocity V used for locating the seismic events by minimizing the difference in location between TLS and seismic events. Similarly, the frequency range used to filter the seismic signals is adjusted by minimizing the error with the TLS location. But you already need an accurate location of the seismic events to associate seismic and TLS events! Where did you start from? How did you deal with ambiguities? This part needs more explanations. Maybe you could select the rockfall seismic signal with the largest amplitude and assume it corresponds to the largest volume detected by TLS, and adjust the seismic wave velocity for this event? Then run the location with this velocity for all events, associate TLS and seismic events, and only latter re-optimize V for all events?*

Reply: Indeed, the section was confusing. One misleading part arose from the optimised frequency section. This has been rewritten, see above. For the rest, in principal we treated our data and approach as if there were no independent TLS-based location constraints. Thus, the second paragraph of chapter 4.4 has also been rewritten to clarify.

Referee 4.10: *In figure 7, the duration of signals does not seem to match the duration listed in Table 2. For instance, events 7 and 9 have duration > 30 s when looking at the spectrograms, but the duration listed in Table 2 is much shorter. Could you add symbols in each PSD plot showing the start and end of each event?*

Reply: The issue has been clarified by explicitly mentioning when a duration was based on the STA-LTA-ratio method (cf. end of section 5.2) versus manually inspecting the waveforms (cf. caption of table 2). In the caption of figure 7 we have now added information about the time axis, i.e., that event start is indicated by the zero tick and duration can be found in table 2, since the end is mainly after a few seconds, which would be tricky to visualise in this figure. The definition of duration does not include subsequent slope activity (e.g., event 8).

Referee 4.11: *Interpretation of seismic signals: impact or detachment? p19. A figure showing a profile of the cliff at the location of the rockfall would be useful to interpret the rockfall signal. Does the topography of the cliff supports the hypothesis of an impact 1.7 s after the initiation phase? I think that the first low-frequency peak ("phase 2") is more likely the detachment phase (elastic rebound) than an impact. Indeed, I have seen such a signal for many rockfalls that occurred under a roof above an over-hanging cliff, with no possible impact before the cliff base, and with a time delay between* *the detachment phase and the impact at the base that is consistent with free fall.*

Reply: The interpretation has been widened to include the possibility of rock detachment and cliff rebound (see also comments by referee 2). The cliff geometry with a few small ledges along the about 88 degree steep topography has been added to the study area description. The main point that would argue against phase 2 being the rebound is that the rock mass, as it reaches the cliff base, does not result in a single strong signal but rather a emergent wave form, which we tend to interpret as a shower of already fragmented rocks. This fragmentation must take place somewhere, and most probably this is phase 2 when the detached rock mass hits the cliff higher up.

Referee 4.12: *You discuss only one event in section 6.3. What about the other 9 events?*

Reply: Indeed, we could discuss other than the one example event. We chose to spotlight only this rockfall because the scope of the manuscript is on comparing the TLS data with the seismic detection and location results to pursue the goals mentioned in the title. A more thorough and rich discussion of seismic insight to rockfall can be found in another manuscript by Dietze et al., also submitted to ESurfD: Dietze, M., Turowski, J. M., Cook, K. L., and Hovius, N.: Spatiotemporal patterns and triggers of seismically detected rockfalls, Earth Surf. Dynam. Discuss., `https://doi.org/10.5194/esurf-2017-20`, in review, 2017. We think that including further rockfalls into this discussion section here would blur the focus or make it difficult to define which ones to include and which ones not. We provide the full seismic data to invite readers to reproduce and explore the properties of other events.

Referee 4.13: *Can you identify fracture, detachment, impact and/or propagation phases? If you see both the detachment and impact phases, do you find a good agreement between the free fall height estimated from the seismic signal and from the source location?*

Reply: Discriminating fracture from detachment is hardly possible with the data of this study, as discussed two points above. Based on the inferred free fall phase explained in figure 2 we indeed find a reasonable agreement of TLS-based detachment height and the cliff base/talus slope, a point we discuss in the second paragraph of chapter 6.3. However, the other manuscript (reference see above) gives a much deeper and more appropriate insight to this topic, based on a larger data set.

Referee 4.14: *Fig 3: Add a scale bar and all plots*

Reply: The images in a) and b) are perspective views, not orthorectivied imagery, which makes it difficult to add globally valid scale bars. We mention now in the figure caption the approximate extent of the cliff stretch and link to figure 1a) where the station distances are given. For c) the pixel sizes are not equal but modified to scale the detachment area for the plot.

Referee 4.15: *Fig 7 : For which station is the PSD computed?*

Reply: Information has been added to the figure caption.

Referee 4.16: *Figure 5 : There are 5 solid lines corresponding to events with $P_{max} > 0.94$. But according to Fig 6 there should be 10 events with $P_{max} >= 0.94$?*

Reply: The usage of the 0.95 quantile threshold and P_{max} was confusing and has been clarified throughout the manuscript, see also comments by other reviewers. With respect to figure 5, there are only five lines because these are the only ones that reached an R^2 for the location estimate above 0.94. This value may not be confused with the quantile threshold used to clip the location estimate polygons, such as the 0.95 quantile or the 0.973 quantile. In the figure, 0.94 was used because the other lines reached significantly lower (< 0.8) values and were not used for the velocity estimate approach. In summary, P_{max}, ΔP_{max}, R^2 and the 0.95 (or 0.973) quantile are now explicitly defined in chapter 4.4 and consistently used throughout the manuscript.

Referee 4.17: *Table 1 : can you add the number of available stations?*

Reply: Basically, the number for all events was four. The overlapping period, when five stations were operating yielded no rockfall event. This number of four stations is now explicitly mentioned in the beginning of chapter 5.2.

Referee 4.18: *Table 2 : Could you also add magnitude (and/or amplitude range) for each rockfall?*

Reply: Table column added as suggested.

~~Validity~~Seismic monitoring of small alpine rockfalls – validity, precision and limitations~~of seismic rockfall monitoring~~

Michael Dietze[1], Solmaz Mohadjer[2], Jens M. Turowski[1], Todd A. Ehlers[2], and Niels Hovius[1]

[1]GFZ German Research Centre for Geosciences, Section 5.1 Geomorphology, Potsdam, Germany
[2]University of Tübingen, Department of Geosciences, Tübingen, Germany

Correspondence to: Michael Dietze (mdietze@gfz-potsdam.de)

Abstract. Rockfall in deglaciated mountain valleys is perhaps the most important post-glacial geomorphic process for determining the rates and patterns of valley wall erosion. Furthermore, rockfall poses a significant hazard to inhabitants and motivates the monitoring for rockfall occurrence in populated areas. Traditional rockfall detection methods, such as aerial photography and Terrestrial Laser Scanning (TLS) data evaluation provide constraints on the location and released volume of rock, but have limitations due to significant time lags or integration times between surveys, and deliver limited information on rockfall triggering mechanisms and the dynamics of individual events. Environmental seismology, the study of seismic signals emitted by processes at the Earth's surface, provides a complementary solution to these shortcomings. This approach is limited amongst others by the strength of the signals emitted by a source and their transformation and attenuation towards receivers. To test the ability of seismic methods to identify and locate small rockfalls, and to characterise their dynamics, we surveyed a 2.16 km^2 large, near vertical cliff section of the Lauterbrunnen Valley in the Swiss Alps with a TLS and six broadband seismometers. During 37 days in autumn 2014, ten TLS-detected rockfalls with volumes ranging from 0.053 ± 0.004 to 2.338 ± 0.085 m^3 were independently detected and located by the seismic approach, with a deviation of 81^{+59}_{-29} m (about 7 % of the average inter-station distance of the seismometer network). Further potential rockfalls were detected outside the TLS-surveyed cliff area. The onset of individual events can be determined within a few milliseconds, and their dynamics can be resolved into distinct phases, such as detachment, free fall, intermittent impact, fragmentation, arrival at the talus slope and subsequent slope activity. The small rockfall volumes in this area require significant supervision during data processing: 2175 initially picked potential events reduced to 511 potential events after applying automatic rejection criteria. The 511 events needed to be inspected manually to reveal 19 short earthquakes and 37 potential rockfalls, including the ten TLS-detected events. ~~Rockfalls do~~ Rockfall volume does not show a relationship ~~to~~ with released seismic energy or peak amplitude at this spatial scale due to the dominance of other, process-inherent factors, such as fall height, degree of fragmentation and distribution, and subsequent talus slope activity. The combination of TLS and environmental seismology provides, despite the significant amount of manual data processing, a detailed validation of seismic detection of small volume rockfalls, and revealed unprecedented temporal, spatial and geometric details about rockfalls in steep mountainous terrain.

1 Introduction

Rockfall is a dominant geomorphic process shaping the steepest slopes and landforms that constitute significant portions of mountainous terrain. Despite their small volumes (10^{-1}–10^3 m^3) in comparison with other mass wasting processes, such as rock avalanches (10^2–10^5 m^3) and rockslides ($> 10^6$ m^3) (Krautblatter et al., 2012), rockfalls can pose a significant hazard, due to their rapid evolution, high velocity and impact energy, and proximity to infrastructure. Thus, precise information on released volume, timing, location, dynamics and triggers is essential for understanding the underlying mechanisms, improving process based models, and to build robust mitigation and early warning systems. The unpredictable occurrence of rockfalls hinders detailed investigation of their dynamics and drivers under natural conditions. Direct observation of events is rare and restricted to, for example, the Yosemite Valley with thousands of camera-equipped tourists per day (Stock et al., 2013). Typical approaches to deliver information about rockfalls are deterministic and probabilistic susceptibility analysis, predictive modelling, a posteriori mapping of detachment zones, released volumes and pathways by aerial and satellite imagery or repeated TLS surveying (Volkwein et al., 2011). The latter technique (Ring, 1963) provides high-resolution spatial data of topographic change attributable to rock detachment ~~(Rabatel et al., 2008; Zimmer et al., 2012; Strunden et al., 2014)~~(e.g., Rabatel et al., 2008; Zimmer et al., 2012; Strunden
but is time consuming during recording and evaluation and primarily suited for longer, monthly to annual lapse times. Over the integration time between two consecutive scans it is possible to identify spatial activity patterns, released volume ranges and magnitude-frequency relationships (Strunden et al., 2014). However, multiple rockfall releases from the same location cannot be resolved. Likewise, the relation between processes and external triggers remains obscured by the relatively coarse time resolution associated with many repeat TLS studies. Hence, insight into the individual stages of a single event (i.e., detachment, fall, impact and disintegration, duration, multiple failures) is impossible.

Seismic methods provide a solution for this shortcoming. Broadband seismometer networks have been used to detect and locate a wide variety of Earth surface processes, such as landslides ~~(Ekström and Stark, 2013; Burtin et al., 2013; Dammeier et al., 2011)~~(e.g.
rockslides and rock avalanches ~~(?Lacroix and Helmstetter, 2011)~~(e.g., Hibert et al., 2011; Lacroix and Helmstetter, 2011), debris flows (Burtin et al., 2014) and bed load transport in rivers ~~(Burtin et al., 2008; Gimbert et al., 2014)~~(e.g., Burtin et al., 2008; Gimbert et
This emerging research field as well as using seismic noise cross-correlation methods to investigate the states and changes of subsurface conditions are referred to as environmental seismology ~~(cf. Larose et al., 2015)~~(Larose et al., 2015). With a few exceptions, the current studies have focused on monitoring activity at catchment or sub-catchment scale, usually either with limited validation against independent data, focusing on detachment volumes above 10^3 m^3, or working under very controlled, laboratory-like experimental conditions.

Combining TLS and seismic data may provide essential and complementary information on rockfall dynamics and characteristics. This could allow assessment of the performance of the seismic approach in terms of correctly identified events, missed events, additional events and spurious events. Further, the combined approach could contribute information beyond the TLS data, such as the existence of rockfalls from the same location but subsequent activity periods or insight into individual stages of a rockfall sequence. In this study, we investigate the validity of environmental seismology to detect and locate rockfall events that are independently identified by TLS surveys in a steep valley of the European Alps. This validation includes exploring the limits of seismic detection in terms of rockfall size and the accuracy of individual event location. Providing a workflow for automatic event detection, location and description is not one of the major goals as it stands in conflict with the above aims focused on small rockfall volumes.

2 Study area

The Lauterbrunnen Valley in the central Swiss Alps is a deglaciated U-shaped valley. It is flanked by up to 1000 m high, Mesozoic limestone cliffs with sometimes almost vertical walls (88.5 °) and several hanging valleys that host more than 70 waterfalls. Talus slopes at the base of the cliff, reaching around 150 m above the valley floor, argue for substantial and sustained rockfall. The steepest wall section separates the town of Mürren above the cliff from the town of Lauterbrunnen in the valley (fig. 1). Our study focused on this wall, which has minimal snow and vegetation cover throughout the year. The wider area contains further rockfall-prone locations that can deliver rockfall signals, such as the steep slopes of the Chänelegg and the ridge south of the Ägertenbach (fig. 1 a). The steep topography of the Lauterbrunnen Valley with a few small ledges (fig. 3 b) implies a significant free fall phase of detached rocks, followed by rockmass impacts on the cliff face or the talus slopes below, perhaps grading into moderate translocation processes on the less than 250 m long depositional areas. Rockfall activity in the Lauterbrunnen Valley has been monitored by repeated TLS since 2012 (Strunden et al., 2014), yielding 122 detected rockfalls (523.72 m^3 in total) over an 18 month investigation period. These events appear to be evenly distributed throughout valley walls (15.13 events per year and km^2) with most frequent events being smaller than 1 m^3.

3 The seismic view on rockfall

The seismic approach to ~~study~~ studying Earth surface processes (fig. 2) utilises the ground motion recorded by a network of sensors. These signals can be studied in the time domain (i.e., time series of ground velocity) and frequency domain (i.e., the frequency spectrum of the entire signal), or in combination (i.e., ~~power spectral density estimates in moving time windows~~spectrograms, stacked spectra of time slices of the signal). A rockfall event manifests as a series of short and long pulses of ground velocity above the ambient background noise level (fig. 2 a), with characteristic frequency contents over the entire frequency band above 5 Hz (fig. 2 b), usually dominated by the 10–30 Hz band (e.g., Hibert et al., 2014). This characteristic pattern makes rockfalls distinct from other seismic sources, such as earthquakes and anthropogenic noise. The individual pulses and their spectral properties can be interpreted genetically, e.g., as successive rock mass impacts, fragmentation and subsequent slope activity ~~(e.g., Burtin et al., 2014; ?)~~(e.g., Burtin et al., 2014; Hibert et al., 2014). Each signal pulse, emitted at a source location, travels predominantly as a surface wave ~~(Burtin et al., 2016)~~ (e.g., Dammeier et al., 2011; Levy et al., 2015; Burtin et al., 2 a finite velocity~~, and thus~~ . Thus, in a homogeneous medium, the seismic signal arrives at different seismic stations at different times ~~. This time offset between~~ and with systematic, frequency- and distance-dependent changes of the signal properties. These property changes can be significantly altered due to heterogeneous rock and structure characteristics in natural environments. Nevertheless, the time offsets with which signals are recorded at the stations allows finding a location in space that best ex-

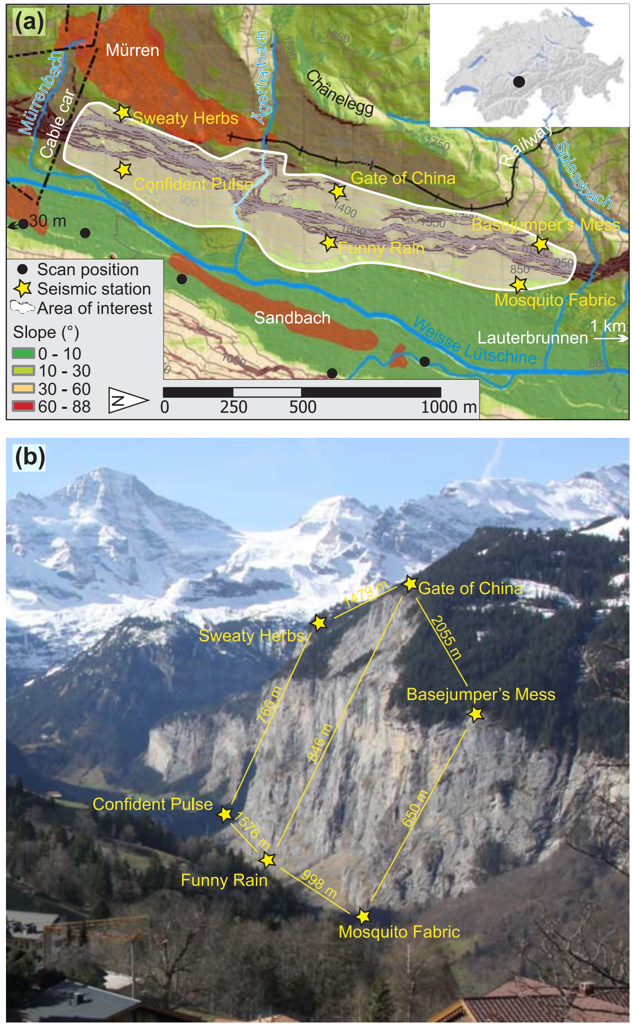

Figure 1. The study area Lauterbrunnen Valley. (a) Schematic map with location of seismic stations, TLS positions and anthropogenic noise sources (settlements, technical infrastructure). (b) Photograph of the instrumented east-facing cliff face of the Lauterbrunen Valley with the Breithorn and Tschingelhorn in the background. Seismic stations (yellow stars) are separated by 1200 m on average.

plains the overall spread of signal arrival times at all stations. Thus, seismic signals have the potential to deliver ~~vital~~ unique, important information about rockfall dynamics and location, if comparison with independent data confirms the validity of the approach. The example of fig. 2 is actually one of the events detected in this study. After the validity of the method has been demonstrated, it will be interpreted genetically to highlight the level of detail that environmental seismology can provide to describe Earth surface processes.

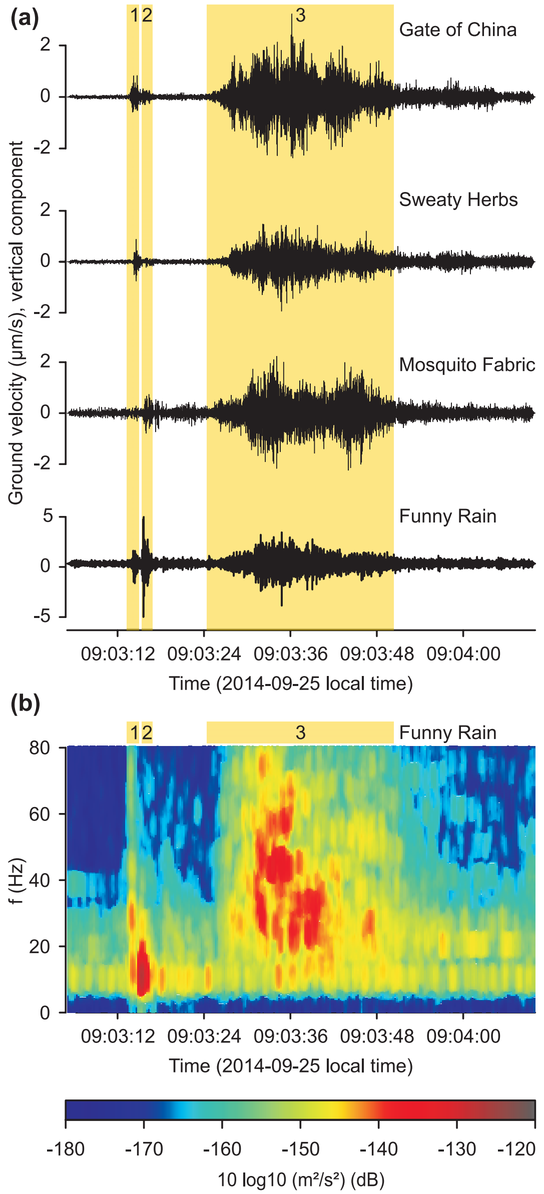

Figure 2. Anatomy of a ~~rockfall event~~0.891 ± 0.038 m^3 large rockfall event (event 7 from table 2). (a) Seismic waveforms (filtered between 1 and 90 Hz) of four stations (see fig. 1 for locations). (b) Power spectral density estimate of station “Funny Rain”. Two distinct, short seismic activity phases (yellow polygons 1 and 2) are followed by an emergent and prolonged period of activity (yellow polygon 3) after 7.5 s of calm.

4 Methods

4.1 Equipment and deployment

High resolution point clouds ~~(~~with a limit of detection (i.e., the smallest resolvable length fraction at the cliff surface) of about 11 cm ~~)~~ were generated by TLS, using an Optech ILRIS-LR terrestrial light detection and ranging (lidar) scanner with a scan frequency of 10 kHz and a reflectivity of 80 % at 3 km distance. Scans were recorded during two field campaigns on 22 September 2014 and 28 October 2014. The TLS data collection and processing approach used in this study is identical to that of previous work conducted in the same study area (for details see Strunden et al., 2014). To ensure sufficient overlap and to avoid topographic shading effects, the study area was scanned from five different positions (see fig. 1 a). Seismic activity was measured by six Nanometrics Trillium Compact 120s three component broadband seismometers. The ground velocity signals were recorded with Omnirecs Cube ext^3 data loggers, sampling at 200 Hz, with gain set to 1 and a GPS flush time 30 minutes. Deployment sites were chosen to optimise the potential for rockfall location along the east-facing rock wall below the town of Mürren. Stations were separated from each other laterally by 1000–2050 m and vertically by 650–850 m. Three stations were deployed along the upper limits of the talus slopes at the cliff base and three stations on top of the cliff (~~cf.~~ fig. 1). Each seismic sensor was installed in a small hand dug pit at 30–40 cm depth. Seismic activity was recorded for 89 days, between 1 August and 28 October 2014. In this study only the period bracketed by the two TLS surveys is used (22 September–28 October). For further analyses a digital elevation model (DEM) of the wider study area with 5 m grid size (swissALTI3D) was used, transformed to the UTM coordinate system and resampled to 10 m grid size.

4.2 Lidar data processing

Point clouds were processed with the "Joint Research Center 3-D Reconstructor 2" software, adjusted manually and merged using control points and a best fit algorithm to minimize differences in the overlapping data. Rockfall detachment locations and volumes were calculated from the two data sets using the inspection tool and the cut and fill algorithm. Photographs recorded during scanning were used to confirm that the detected volume changes were not caused by processes other than rockfall (e.g., vegetation growth). Measurement uncertainty was estimated based on scan differences from stable control regions (for details see Strunden et al., 2014). Detachment area coordinates were obtained by georeferencing the rasterised point cloud data on referenced topographic maps and orthoimages. Given the typical rockfall volumes < 1 $\cancel{m^3}$ m^3 (Strunden et al., 2014), location uncertainty should mainly result from the georeferencing process and is quantified by the root mean square error (RMSE). All location coordinates were rounded to the full meter and transformed to the UTM coordinate system.

4.3 Seismic data processing: Event detection

A single seismic station records 200 samples per second and ~~spatial~~ geometric signal component, resulting in more than 311 million measured values per day. Hence, potential rockfall events must be identified (picked) automatically from the stream of data. However, for rockfall events with volumes usually below 1 m^3 (Strunden et al., 2014) it is challenging to find reasonable parameter settings for any picking algorithm. Therefore, the seismic time series of all operating stations were manually screened during a control period, 22 September–1 October, to find reference events for parameter definitions.

We used an STA-LTA-ratio algorithm ~~(Havskov and Alguacil, 2006)~~(Allen, 1982), calculating the continuous ratio between a long term average (LTA) and a short-term average (STA) of the signal envelope~~(i.e., the absolute value of each measurement)~~. When the onset of an event is recorded it will not affect the LTA value but have a significant effect on the STA value, thus increasing the ratio. When the seismic signal returns to background, the STA values approach the LTA value again, which lowers the ratio towards one. The STA-LTA-ratio picker thus has four relevant parameters: the lengths of the STA window and LTA window, a threshold value to define the start of an event and another threshold value defining the end of an event.

In the case of the Lauterbrunnen Valley the STA window was set to 0.5 s and the LTA window to 180 s, ~~similar to the values~~ based on the experiences of Burtin et al. (2014) from another steep mountainous catchment~~(Burtin et al., 2014)~~. The window lengths obviously affect the number and timing of the initially picked events. Thus, to be sensitive to short lasting and low magnitude rockfall events, we used this short STA versus long LTA value. The threshold values for defining the event start and end were adjusted based on manually identified events from the control period (cf. chapter 5.2). The LTA value was set to constant after an event onset to avoid spurious changes of the ratio for long lasting events (Burtin et al., 2014).

The ~~STA/LTA~~ STA-LTA-ratio algorithm was applied to the bandpass-filtered (third order Butterworth filter) envelope of the vertical component signal of the central cliff top station "Gate of China" (~~cf.~~ fig. 1). The filter cut-off frequencies were set to 10 and 30 Hz to isolate the typical frequencies of rockfalls and rock avalanches ~~(Helmstetter and Garambois, 2010; Zimmer et al., 2012; ?; Bur~~ Since a significant rockfall should be detected by more than one station we require that all events interpreted are identifiable at this central station. Furthermore, this station was chosen because of its remote location, away from potential sources of anthropogenic and fluvial noise, in order to reduce the initial number of spurious detections. Events that were not co-detected by at least two other stations within a time window of 1.75 s were removed from the data set. The value of 1.75 s corresponds to the maximum travel time of a seismic S-wave within the entire seismic network when using a low S-wave velocity in limestone of 2000 ms^{-1} (Bourbie et al., 1987). ~~Also~~This value is also similar to the apparent velocities of local earthquakes and rockfalls as discussed by Burtin et al. (2009) and Helmstetter and Garambois (2010). In principal, a rockfall event can consist of multiple block releases and impacts, and subsequent hillslope activity, all at different locations. Not accounting for such effects by setting the 1.75 s criteria would introduce artifacts that bias the subsequent location approach. Similarly, if two consecutive picked events showed a time offset smaller than 12.8 s, then only the first one was kept. This ensured that rockfalls with multiple impacts were not identified as separate events. However, this also implies that in the case of two unrelated rockfalls, occurring within this time window, the latter one would be ignored. The selected value of 12.8 s corresponds to the maximum possible free fall time of a rock mass from the top of the highest cliff part.

Further options ~~used~~ to reduce false detections ~~are~~ can be to set thresholds for minimum and maximum event duration, signal amplitude variance throughout the network, comparison with existing catalogues (e.g., the Swiss earthquake catalogue), and signal-to-noise (SNR) ratio ~~(cf. Burtin et al., 2014, 2016)~~(Burtin et al., 2014, 2016), the latter being the ratio of the maximum and average value of the signal envelope of an event. However, all these thresholds must be adjusted to an existing data set of potential rockfall events and their effects should be inspected. For the subsequent analysis, minimum and maximum duration as well as SNR ratio were used as rejection criteria, with parameters adjusted based on the control period (cf. chapter 5.2).

The waveforms of all remaining events were inspected manually for plausibility, validity and the possibility to locate their source. This included the following criteria (~~cf. fig~~see fig. 2 for an example of how the criteria are matched): i) ~~signals must be present in at least three records, ii) they must show a time offset corresponding to the minimum and maximum station distance (1.75 s, see above), iii)~~ they should not exhibit the typical features of earthquakes, such as distinct P- and S-wave arrivals, a long coda (i.e., the exponentially decaying tail of the signal), frequencies below 2 Hz, and similar amplitudes at all seismic stations for low frequencies, ~~iv~~ii) they must show ~~a systematic relationship of decreasing signal amplitude with increasing distance from source to sensor and v~~significant differences in signal amplitudes due to the source receiver distance-related attenuation within the network iii) they should either exhibit the presence of one or more erratic peaks in the seismogram as the result of impulsive impacts (Zimmer and Sitar, 2015) or show an avalanche-like emergent signal, i.e., several seconds rise time of the signal from background, followed by a long decay into background noise after reaching a maximum amplitude ~~(Vilajosana et al., 2008; Zimmer et al., 2012)~~(e.g., Suriñach et al., 2005; Vilajosana et al., 2008; Zimmer et al., 2012). The temporal evolution of potential event signals was further inspected using power spectral density (PSD) estimates. These were calculated according to the method of Welch (1967) with moving time windows of 1.4 and 1.1 s to generate the spectra, each with an overlap of 90 %, and the individual spectra were corrected using the ~~multiptaper~~ multitaper method. Rockfall events typically exhibit a burst of seismic energy over a wide frequency range during the first impulsive impact, possibly followed by subsequent activity in the 10–30 Hz frequency band ~~(Vilajosana et al., 2008; ?)~~(Vilajosana et al., 2008; Dammeier et al., 2011; Hibert et al., 2011). The detected potential events should agree with these observations. All successfully evaluated events were used for subsequent analyses.

4.4 Seismic data processing: Event location

Locating the source of the seismic signals emitted by rockfalls can be challenging due to the emergent onset of events, superposition of many impact signals, significant high-frequency content, missing constraints on specific seismic wave types and differences between waveform properties at different stations. The latter is due to the preferential signal attenuation of higher frequency waves, fragmentation of rocks during impact and changing amplitudes with time due to the moving source approaching or passing by a station ~~(cf. Burtin et al., 2013, 2016). Thus, previous approaches of source location based on first arrival times (e.g., ?) cannot be used here. Burtin et al. (2013) describe an alternative technique termed signal migration that we employed for source location. This approach is based on migration of a full seismic waveform through a spatial grid of potential locations and cross-correlation of the signal envelopes,~~ (Burtin et al., 2013, 2016). Approaches that use the full waveform (Lacroix and Helmstetter, 2011) or its envelope (Burtin et al., 2013) are more appropriate to locate the source of seismic signals resulting from such processes. They are based on calculating average cross-correlations of signal pairs, each shifted by the time delay ~~they experience~~ experienced due to the distance of a grid ~~point~~ cell to a seismic station. The grid ~~point~~ pixel with the highest overall correlation value is deemed to be the most likely source location. ~~This probabilistic approach~~ When encountering moving sources, signal migration needs to be performed for each impact signal separately to avoid "smearing" of the location estimate. The probabilistic signal migration approach further requires constraints on the average seismic wave velocity within the area of interest, a suitable frequency window for processing the signals and a topographic correction of the ray paths ~~(cf. Burtin et al., 2013)~~(Burtin et al., 2013).

Velocity tests were performed with two approaches. For all ~~picked~~ 37 picked potential rockfall events the seismic wave velocity within rock was changed between 700 and 4000 ms^{-1} to inspect its influence on the average cross correlation strength of the signal envelopes at different stations. In a second~~step, using~~, independent approach we used the TLS-based rockfall detachment locations ~~,~~ to evaluate the effect of the different wave velocities considered~~(700 and 4000 ms^{-1}) was evaluated~~ , based on the average difference between the seismic and TLS locations. This second approach is only possible when independent information of rockfall locations are present and can also be seen as a validation of the first approach.

~~The~~ Similar to the velocity, the frequency band used in the location routine can have ~~a strong~~ an influence on the location estimate. Both parameters are interconnected and may be optimised with respect to the overall highest cross-correlation value of the location estimate. However, in this study the average seismic wave velocity is regarded a global, spatially and temporally constant parameter and was not adjusted for different frequency bands. For rock avalanches along the steeply inclined slopes of the Illgraben catchment and a widely distributed network of nine seismometers, Burtin et al. (2013) chose the frequency window with the highest signal-to-noise ratio. In the case of the Lauterbrunnen Valley, the seismic signals were much more heterogeneous among the stations. There was no common frequency with high signal-to-noise ratio at all stations. Hence, we used fixed windows of 5–15, 10–20 and 15–25 Hz, depending on the dominant frequency range of the first impact signals. Usually, an event could be located at comparable positions with all three frequency windows. In that case, the window with the highest cross-correlation value was chosen. In cases where none of the three windows resulted in a stable location along the cliff face or other potential rock release zones inside the study area, the frequency windows were adjusted manually based on the dominant frequency range in the PSD. In a second step, the frequency windows of all events were subsequently adjusted manually to minimise the difference between the seismic and TLS-based location estimates of rockfall events~~in order to investigate the maximum possible accuracy of the approach~~. Obviously, this optimisation is only possible when independent location constraints are present and will have different frequency values for each event. Thus, it is used here to evaluate the appropriateness of the fixed frequency window approach and to explore the maximum possible location precision available with the data, methodology and landscape setting of this specific experiment.

Topography correction is necessary ~~for source location because the seismic waves propagate from a source to the seismic stations either along a direct seismic path (within bedrock) or along the surface, when the direct path would be through air (?Lin et al., 2015). This approach assumes that seismic signals emitted by rockfalls , and other Earth surface processes , are dominated by surface waves rather than body waves (Burtin et al., 2016)~~because rockfalls and other gravitational mass wasting processes generate surface waves that propagate following the topography (Dammeier et al., 2011; Hibert et al., 2014; Lin et al., 2015; Bur
The results of this correction were stored in distance maps. These are station-specific grids of the same resolution as the input DEM (10 m) where the cumulative direct distance of each pixel to a seismic station has been modified by that part where the direct distance ~~is~~ was above the actual surface elevation (Burtin et al., 2014). Specifically, the distance between each pixel and station is approximated as a straight line of pixel-sized segments in three dimensional space (xyz vectors) and whenever the

z value (elevation) of a segment is above the DEM-based z value, it is replaced by the latter. The final distance is calculated as the sum of vector magnitudes. To ensure that topographic modification of the wave path is resolved, it is important that the wavelength (i.e., the ratio of wave velocity and frequency) is several times smaller than the average distance between seismic source and the recording station. For typical ~~S-wave~~ wave velocities in limestone between 2000 and 3300 ms~~$^{-1}$ (Bourbie et al., 1987)~~ $^{-1}$ (Bourbie et al., 1987; Helmstetter and Garambois, 2010) and useful frequencies of ~~10–20~~ 10–30 Hz, the wavelengths are a few hundred metres, which is adequate for the average distance between seismic stations (~~cf.~~ fig. 1 b).

All picked events were clipped with a buffer of 3 s before and after the event and then migrated. Locations with a ~~likelihood quantile below~~ cross-correlation value R^2 below the 0.95 quantile were removed and the remaining values were normalised between 0 and 1. Events located along the margin pixels of the distance map of the study area were rejected. Only events inside the area of interest (~~cf.~~ fig. 1) were used for validation. The threshold quantile value of 0.95 to clip location areas is arbitrary though in the range of values from the literature ~~(cf. Burtin et al., 2014)~~(Burtin et al., 2014). To investigate the effect of varying this value on the number of rockfall locations inside the resulting uncertainty polygon was tested by changing the value from 0.9–1.0 and recording the number of TLS-based detachment locations and corresponding downslope trajectories, which remained inside the uncertainty polygons.

Location differences ΔP_{max} were calculated as the minimum planform Euclidean distance between the highest value of the seismic location estimate (P_{max}) and the downslope trajectory line of the corresponding TLS-based detachment pixel. The direction of the trajectory line was defined by the average cliff face azimuth (99 ± 44°). This approach was chosen because seismic signals can only be emitted at the detachment zone or rockfall impact sites below it, and since the cliff face is nearly 90° steep there is a high likelihood that the rock mass will follow the line of steepest descend without much deviation. Uncertainties arising from deviations of the rock mass from this line cannot be accounted for.

All seismic analyses were performed in the R environment for statistical computing (R Development Core Team, 2015) (version 3.3.1) using the packages eseis (Dietze, 2016), sp (Pebesma and Bivand, 2005; Bivand et al., 2013; Pebesma and Bivand, 2016) and raster (Hijmans, 2016).

5 Results

5.1 Lidar-detected rockfalls

Between 22 September and 28 October, ten rockfall events were detected by TLS. The events were spread over the entire monitored part of the cliff, but the southern section, near stations “Sweaty Herbs“ and ”Confident Pulse“, hosted 50 % of all events. The smallest detected rockfall (event 5 in table 1) had a volume of 0.053 ± 0.004 m^3 while the largest rockfall (event 10 in table 1) had a volume of 2.338 ± 0.085 m^3. The average volume of rockfalls in this period was 0.482 m^3. A summary of all rockfall events including location coordinates based on TLS and seismic data is shown in table 1. With only one exception (event 6), all rockfalls detached from the lower part of the cliff, some almost at the base (~~cf.~~ fig. 3 b, table 1). The georeferenced RMSE in the event locations was between 4.8 and 17.5 m. The range in RMSE values calculated depends on the number of identified ground control points (between 8 and 17 per scene) as well as the size and perspective of the referenced image.

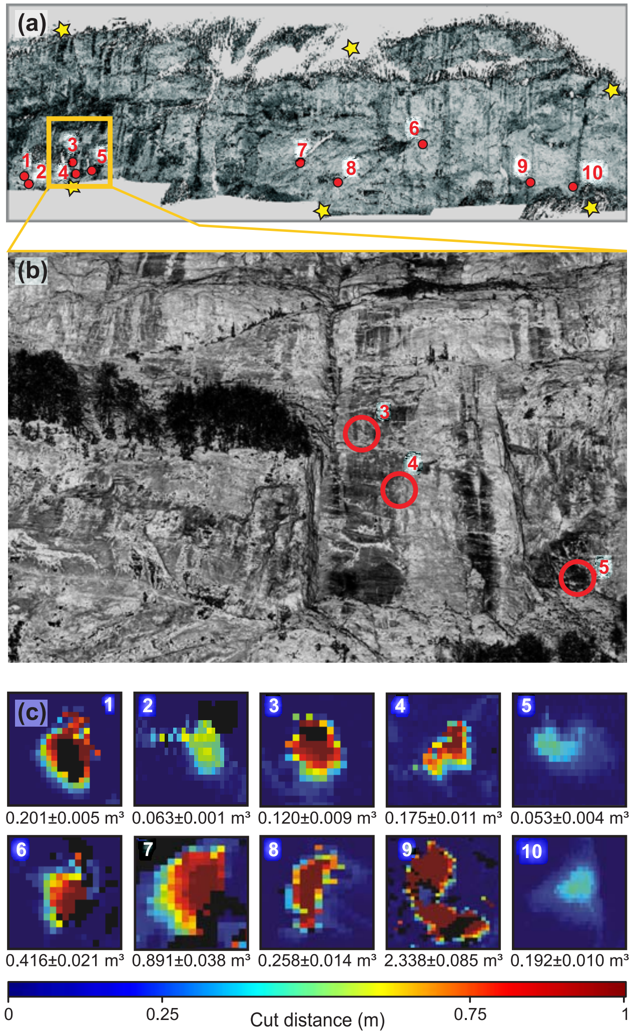

Figure 3. Rockfall detachment zones determined from TLS mapping. (a) Overview (aligned point cloud data) of the about 2.7 km long, instrumented east-facing ~~wall~~ stretch of the Lauterbrunnen Valley with rockfall detachment zones (red dots) and seismic stations (yellow stars, station names and distances see fig. 1). (b) Close-up of the southern rock wall section with the detachment zones of events 3 ~~-~~ – 5 at elevations less than 100 m above the talus slope. (c) Boxes show rockfall detachment patterns on the rock wall. Released rock volumes and uncertainties are given below each box. Event numbers are the same as in (a) and tables 1 and 2)

.

5.2 Continuous seismic data processing

Over the entire monitoring period there were always at least four seismic stations operating simultaneously. ~~The~~ Due to topographic shielding, the basal stations needed several days after deployment and maintenance to receive a GPS signal,

Table 1. Rockfall location summary. Subscript TLS denotes UTM coordinates from aligned TLS point cloud data. Subscript seis denotes coordinates based on seismic signal processing, i.e., site/point of the highest location probability (P_{max}). Ranges of z-coordinates are determined as min-max range of a 3 by 3 pixel matrix around the detected location. P diameter is the greatest lateral diameter of the location uncertainty polygon (~~cf.~~ fig. 8). ΔP_{max} is the deviation of the most likely seismic location estimate from the rockfall trajectory as determined from TLS surveys. The values outside brackets give deviations ~~after optimisation~~with default settings, values in brackets give ~~the default deviation~~smallest possible deviations with optimised location frequency windows (only possible when independent location data is available).

ID	x_{TLS} (m)	y_{TLS} (m)	z_{TLS} (m)	V_{TLS} (m^3)	x_{seis} (m)	y_{seis} (m)	z_{seis} (m)	P diameter (m)	ΔP_{max} (m)
1	415511	5156535	964–1036	0.201 ± 0.005	415485	5156551	1063–1119	860	760 (31)
2	415523	5156542	952–1022	0.063 ± 0.006	415505	5156541	1005–1063	792	50 (18)
3	415541	5156844	1084–1138	0.201 ± 0.005	415515	5156841	1141–1192	943	27 (27)
4	415566	5156845	1018–1100	0.175 ± 0.011	415505	5156871	1184–1218	968	92 (66)
5	415591	5156934	1009–1062	0.053 ± 0.004	415635	5156991	999–1054	587	147 (63)
6	415950	5158213	1170–1314	0.416 ± 0.021	415965	5158241	1182–1224	687	21 (21)
7	415952	5157829	1048–1123	0.891 ± 0.038	416015	5157781	907–927	858	117 (37)
8	416005	5157897	916–1026	0.258 ± 0.014	416015	5157891	889–954	614	251 (4)
9	416116	5158797	919–1002	0.192 ± 0.010	416065	5158811	1117–1217	498	70 (53)
10	416037	5158649	979–1114	2.338 ± 0.085	416095	5158691	922–939	361	60 (52)

necessary for time synchronisation~~, due to topographic shielding~~. Two seismic stations failed during the monitoring period (“Basejumpers Mess” on August 29 and “Confident Pulse” on September 27), due to progressive sensor tilting caused by slope movement or sediment settling. However, the remaining stations provided sufficient data for detection and location of events, i.e., all event descriptions are based on data from four seismic stations.

Manual screening of seismic records during the control period (22 September and 1 October) yielded evidence of two rockfalls, events 7 and 10 of the final data set (table 2). One of these rockfalls (event 7, fig. 4 b) generated two short, distinct bursts of seismic energy, less than 2 s apart, followed by a rise of the seismic signal about 7.5 s later (~~cf.~~ see fig. 2 for details). The first burst contains frequencies between 30 and 60 Hz, while the second peak mainly has frequencies below 20 Hz. The subsequent strengthening signal is again dominated by frequencies between 30 and 80 Hz. The entire sequence was recorded by all operating stations, though with different amplitudes, from about ± 0.38 ~~μms^{-1}~~ $\mu\mathrm{ms}^{-1}$ at station “Sweaty Herbs” to ± 4.9 ~~μms^{-1}~~ $\mu\mathrm{ms}^{-1}$ at station “Funny Rain”. The maximum time offset between event onsets at the stations was 0.51 s. The ~~STA/LTA~~ STA-LTA-ratio values reached up to 7 for the first two peaks and decreased below 2 before grading to the next rise.

Based on the above characteristics of event 7 and similar properties for event 10 from the control period, the parameters for event picking of the entire data set were defined~~. The STA/LTA~~, i.e., the STA-LTA-ratio threshold to define the start of an event was set to 5, the threshold for defining the end of an event to 3. Note that this approach does not yield a correct start and

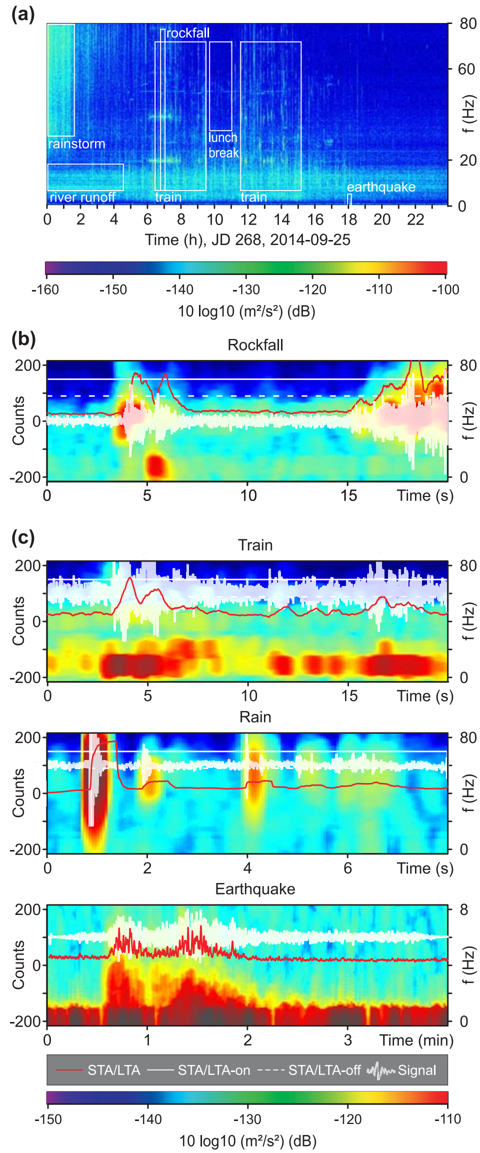

Figure 4. Example day (~~September~~ 25 September 2014) showing seismic characteristics of environmental sources in the Lauterbrunnen Valley. (a) 24 h PSD with interpreted sources indicated. Data recorded at station “Mosquito Fabric” and filtered between 1 and 90 Hz. (b) Seismic record of rockfall event 7 (~~cf.~~ table 2). (c) Seismic records of other sources registered by the station “Gate of China”. Note change in axes scales for the earthquake event. (b) and (c) contain the PSD (background image, colour bar applies to (b) and (c)) and waveform data (semitransparent line graph) as well as the picker algorithm characteristics (STA-LTA-ratio~~as well as~~, “on”- and “off”-thresholds).

end time. However, the location approach is not based on exact onset times but is used with the addition of a 3 s wide buffer before and after an event. The minimum SNR of an event at the picking station “Gate of China” was set to 6.

The instrumented study area comprises many further environmental sources that generate seismic signals with frequencies above 1 Hz. Fig. 4 a shows a 24 h PSD as an example. From 4 ~~am–9~~ am to 9 pm (UTC time, i.e., ~~+ 2~~ -2 h to local time) there are pulses of seismic activity in the 5–80 Hz range, occurring every 20 minutes. Until 2 am there is continuous activity with frequencies above 30 Hz and over the day there is a progressively decreasing signal between 5 and 15 Hz, which in general depicts the runoff of the Weisse Lütschine (FOEN, 2017), the main river draining the Lauterbrunnen Valley, and is in agreement with the seismic signature of turbulent water flow (Gimbert et al., 2014). Around 2:45 am, 5:10 am and 5:50 pm and 6:05 pm there are seismic events with very low frequency content (maximum energy below 2 Hz). Fig. 4 c shows that the seismic properties of all these other sources can be very similar to the waveforms of rockfalls. Between 4 am and 9 pm (UTC time) a train runs every 20 minutes between Mürren and the cable car station of Lauterbrunnen. The passage of this train is recorded in a repeating succession of spikes of seismic energy in the PSD from fig. 4 a. Although this signature is easily discernible because it repeats at expected times during the day (i.e., Swiss trains ~~alyways~~ always run on time), it also shows two distinct peaks that cross the ~~STA/LTA~~ STA-LTA-ratio start and end thresholds for rockfall detection, and it shows similar amplitudes and amplitude differences between the recording stations. Also the SNR values are comparable with those of rockfalls. The second panel of fig. 4 c shows the impact of rain drops on the ground above the seismic sensor. Attribution of this signal to rain drops is based on the ~~observation that it only occurs in the record when it was raining in the Lauterbrunnen Valley during deployment and maintenance of the stations.Also, these signals were strongest at stations deployed below a tree cover that allows collection of small droplets and release as large drops.~~ notion that these irregular short pulses only occurred during rainy conditions (fig. 5 a and b) and, furthermore, were predominantly registered by stations under forest cover in contrast to sensors deployed at grass covered sites (fig. 5 c versus d). We attribute this phenomenon to trees collecting small rain drops and releasing them after some time as larger drops. Trees continue to release such drops even after the atmospheric rain input has stopped. In contrast, grass covered areas receive the precipitation directly and are subject to systematically smaller drops, especially during gentle rain events. The irregular occurrence of the seismic pulses make an origin due to passing animals or humans unlikely, as one would expect a growing and decreasing amplitude during approaching, passing and leaving the station (a signature inherent to many base jumpers hiking past the stations on top of the cliff during sunny days). The signal of a raindrop is also similar to the rockfall signal although it contains seismic energy over nearly the entire frequency range and lasts less than half a second. Such signals can trigger the ~~STA/LTA~~ STA-LTA-ratio algorithm if they were recorded by chance at more than two stations within the defined maximum ~~lag time~~ time window of 1.75 s. The last panel of fig. 4 c shows an earthquake. The signal of this tele-seismic event is dominated by frequencies below 4 Hz and lasts more than one minute. There are also local earthquakes in the seismic records that show a more sudden onset, contain higher frequencies and last much less than a minute. But all earthquake signals are clearly different from rockfalls. Their waveforms usually show the distinct arrivals of P- and S-waves and ~~the exponentially decaying~~ a coda, their PSDs exhibit a significant portion of energy below 10 Hz, and their waveforms and spectral properties are relatively uniform among records of the different seismic stations.

Thus, to eliminate false events picked by the ~~STA/LTA~~ STA-LTA-ratio approach the minimum duration of an event was set to 0.5 s to remove rain-related picks and the maximum duration was set to 20 s to remove earthquakes. ~~Additionally, the~~ The minimum average SNR value among all stations was set to 6. The ~~STA/LTA-picking~~ STA-LTA-ratio approach yielded a total of

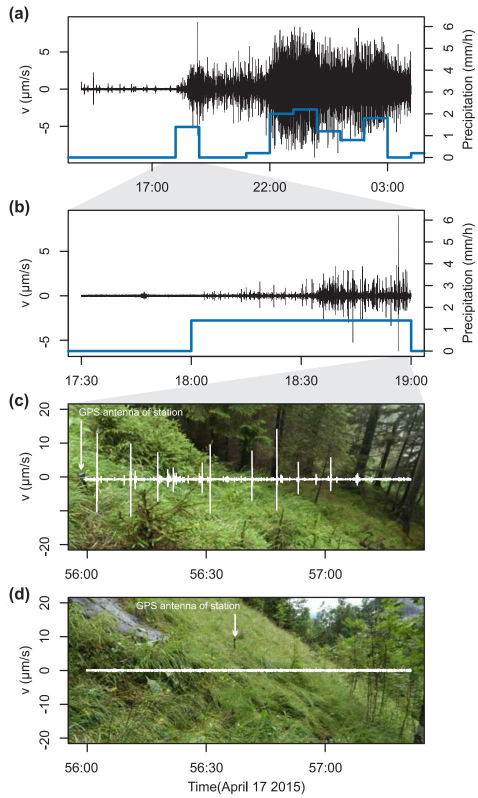

Figure 5. Seismic signal characteristics during a gentle rain event without windy conditions (hourly meteorological data from Meteomedia station in Mürren). Panels a to c show the vertical component signal (filtered between 1–90 Hz) of station “Basejumpers Mess”. Panel d shows the same time interval as c but for station “Funny Rain”. Background images of c and d show the deployment situation of the two stations under a dense coniferous forest cover and on grass land, respectively. Note overall increase in seismic signal amplitudes during the rain event and and short irregular signal pulses only under forest cover, interpreted as impacts of large drops collected and amalgamated by the trees. Trees continue to release drops even after the precipitation record shows no further atmospheric rain input (a).

2175 potential events. After application of the automated rejection criteria the number decreased to 511. These 511 events had to be manually screened and included 455 spurious or unknown events, 19 short earthquakes and 37 potential rockfall signals. The most common spurious event type was associated with train traffic. This type of signal could not be eliminated by any automatic routine and had to be removed manually. The remaining earthquakes had an average STA-LTA-based duration of $11.9^{+4.6}_{-4.0}$ s (median and quartiles) and were also removed manually. The 37 detected potential rockfall events had STA-LTA-based durations of $4.7^{+2.8}_{-2.0}$ s. Several of the potential rockfall events had very weak seismic signals, with average SNRs below 8 (~~n = 8~~eight cases) but the majority generated average SNRs of $11.2^{+2.8}_{-2.6}$. ~~Although the SNR of an event is somewhat related to its duration, this relationship is rather weak (r = 0.37). Likewise, the correlation coefficient between SNR and the log of the maximum signal envelope amplitude (246^{+138}_{-108} counts) is not higher than 0.44.~~

Table 2. Rockfall events detected by seismic monitoring. IDs correspond to those in table 1. Duration as estimated from signal wave form interpretation (not including subsequent talus slope activity). SNR denotes range of signal-to-noise ratios among all recording stations. $f_{default}$ describes the default frequency range for location, f_{opt} denotes the frequency range after optimisation. A is the amplitude range among the stations.

ID	Time (UTC)	duration (s)	SNR	$f_{default}$ (Hz)	f_{opt} (Hz)	A (nms^{-1})
1	2014-10-12 22:45:50	1	8.7–25.9	10–20	10.0–23.0	1356–11945
2	2014-10-15 01:58:32	4	5.2–49.4	10–20	11.0–21.0	1062–4128
3	2014-10-20 19:11:09	5	10.7–35.8	10–20	10.0–20.0	619–2405
4	2014-10-20 15:05:34	7	14.0–55.86	15–25	16.0–26.0	722–3229
5	2014-10-22 11:47:28	2	5.7–11.9	10–20	11.0–19.9	1442–3831
6	2014-10-02 17:59:50	4	6.48–11.76	5–15	5.0–16.0	1055–2077
7	2014-09-25 07:03:13	6	7.5–19.9	10–20	2.8–5.6	962–5980
8	2014-10-26 20:08:45	2	6.0–14.2	10–20	7.0–13.0	1277–306905
9	2014-10-17 00:09:25	8	5.5–11.1	5–15	4.7–15.2	828–1806
10	2014-10-01 09:23:05	10	17.0–59.1	5–35	1.0–35.0	3123–4491

5.3 Seismic wave velocity estimate

A necessary step for successful location of the potential rockfall events ~~is~~ was to find a plausible estimate of the average seismic wave velocity (fig. 6). Both approaches, optimising the average location ~~R^2~~ estimate value (i.e., R^2 at P_{max}) and minimising the difference between seismic location and TLS-based coordinates, point at a common value around 2700 ms^{-1}. While for the latter approach the velocity range with minimum offsets is narrow, with not much argument for an uncertainty range, there is no such clear result for the former approach. The solid black lines in fig. 6 show two velocity ranges with high P_{max} values, between 1000 and 1800 ms^{-1} and between 2200 and 3000 ms^{-1}. Due to the recent deglaciation and persistent rockfall activity, the limestone cliffs of Lauterbrunnen appear rather compact and only marginally weathered. Thus, there is no reason to assume much lower values than those of 2000–3300 ms^{-1} for S-waves in limestone from empiric tests (Bourbie et al., 1987). Accordingly, the first local maximum at lower velocities did not yield any consistent rockfall locations along the cliff, even when the other criteria clearly pointed at a rockfall. The average ~~P_{max}~~ R^2 values for the higher velocity range from a broad plateau of equally likely velocities including 2700 ms^{-1}. Thus, based on information from both approaches, the average seismic wave velocity for running the location routine was set to 2700 ms^{-1}. Without the existence of independent locations of rockfall detachment zones, seismic velocity can only be constrained with low uncertainty by active seismics.

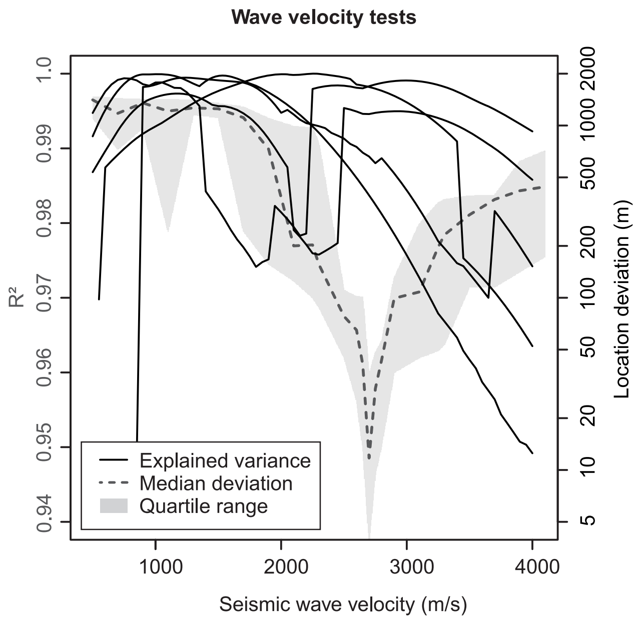

Figure 6. Tests of the most likely average seismic wave velocity. Black solid lines show location ~~quality (~~approach correlation coefficient (average of all R^2) for velocity values ranging between 700–4000 ms^{-1} for all events ~~with $P_{max} > 0.94$~~that reached an $R^2 > 0.94$. Dashed grey line (median) and shaded area (interquartile range) depict deviation of seismically detected from TLS-based event locations. Both measures point at 2700 ms^{-1} as the most likely average seismic wave velocity in the study area. The secondary ~~P_{maxm}~~ R^2 maximum at lower velocities did not yield locations inside the area of interest despite high ~~P_{maxm}~~ R^2 values.

5.4 Location of rockfalls

Applying the location routine to the 37 potential rockfall events placed nine of them in the area of interest covered by our TLS surveys and the seismic network (~~cf.~~ fig. 1). Eight further events were located along the west-facing valley side. Most of these had poor location constraints due to low SNR or inappropriate fits of the overall time delays of the signal envelopes. The other events could either only be located along the margins of the distance maps as the closest approximation for more distant sources, or were located west of the Lauterbrunnen Valley, higher in the catchment. One event, which showed all characteristics of a very proximal rockfall and subsequent rock avalanche but exhibited an extraordinarily wide frequency range (~~cf.~~ event 10 in fig. 8) could successfully be located within the area of interest by manually setting the location frequency window to 5–35 Hz.

Thus, after extensive processing and manual verification, all ten TLS-detected rockfalls could be independently located by the seismic approach. SNRs of all ten events were above 5 and up to 59, depending on the magnitude of the event and the distance of the source to a seismic station. With the exception of the manually adjusted settings for event 10, the default settings resulted in an average difference between TLS (i.e., line of steepest descend from detachment zone) and seismic location of

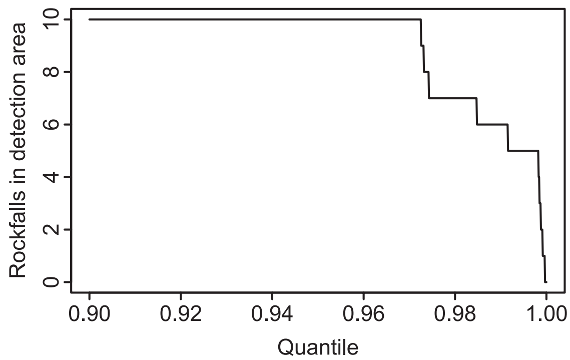

Figure 7. Number of rockfall trajectories inside location estimate polygons as function of minimum location estimate quantile.

81^{+59}_{-29} m. The maximum difference was 761 m (event 1, ~~cf~~ table 1) because a significant part of the location estimate polygon for this event, including the location of P_{max}, was placed on the other valley side, separated from the cliff face by the entire valley floor. However, all TLS-based events were located within the default ~~95 % threshold uncertainty areas~~ uncertainty areas defined by the 0.95 quantile, most of which were elongated by several 100 m in the north-south direction in plan view (~~cf.~~ table 1). Some areas of uncertainty extend into the valley floor (events 6–8) but most were entirely within the cliff face. In five of the ten cases, P_{max} is located higher on the cliff than the TLS-based detachment zones (i.e., events 1, 2, 3, 4, 9). We see the main causes for deviations in inhomogeneities of the solid media, resulting in spatially non-uniform seismic velocities. Specifically, there should be a velocity difference between the solid limestone that forms the cliff and the debris fabric that constitutes the talus slopes. Thus, especially impact locations close to or at these talus slopes may be affected by larger deviations because the average seismic velocity successively fails to explain the arrival times of signals at the seismic stations.

Adjusting the frequency windows for the location routine to minimise the differences to the TLS data usually required shifts by less than 4 Hz. Events 7 and 8 required greater adjustments, as low-frequency windows yielded much better results (~~cf.~~ table 2). Optimising the location settings resulted in average location differences of 33^{+20}_{-6} m with a maximum deviation of 66 m and a minimum deviation of 4 m.

Increasing the quantile thresholds to define the uncertainty polygons for each location estimate reduces their area, which eventually leads to a drop of the number of matches with TLS-based event location (fig. 7). Up to a threshold value of ~~0.9726~~0.973, all ten rockfalls are included in the uncertainty areas.

6 Discussion

6.1 Rockfall detection from continuous seismic data

The challenge of detecting rockfalls with the seismic approach is to identify a few short target signals in month-long records of hundreds of samples per second. This is especially relevant for the small rockfall events of this study. Thus, the described

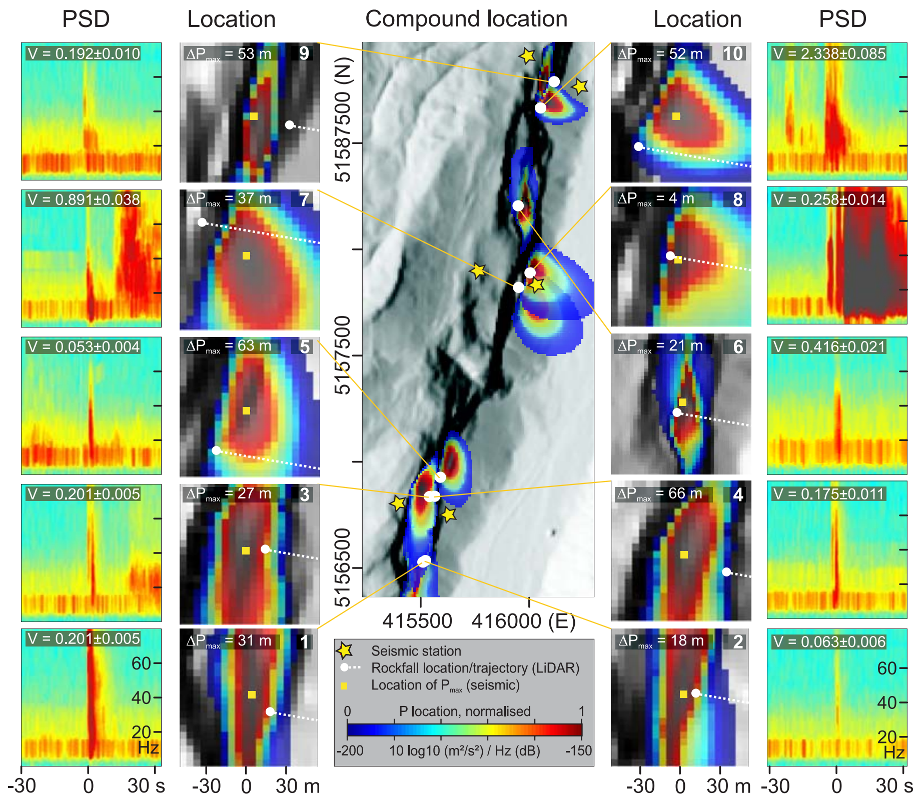

Figure 8. Seismic location of the 10 TLS-based rockfall events. Compound location map shows an overlay of all 10 detected events with coloured polygons corresponding to ~~location likelihood $P > 0.97$~~locations with cross-correlation values above the 0.973 quantile. Location close-up boxes are centred at P_{max}, i.e., the location with the highest ~~location likelihood~~cross-correlation value. PSD boxes show the spectral evolution of each event as recorded by station "Funny Rain". Event start is indicated by time zero. For event duration see table 2. ΔP_{max} is the deviation of seismic location estimate from rockfall trajectory along steepest path. Locations of all rockfalls shown based on optimised location frequency windows for illustrative reasons (table 1 for default deviations).

data processing routine is neither intended to be nor capable of coming close to automatic detection and location of rockfalls of this size. The work flow of signal processing and analysis significantly reduced the number of initially picked events by a factor of 4. This provided a reasonable base for the subsequent manual identification of likely rockfall events. The ~~STA/LTA~~ STA-LTA-ratio threshold values (i.e., 5 and 3) as well as the SNR threshold value (i.e., 6), determined from the two manually identified events in the control period, allowed detection of all ten rockfalls shown by the TLS data, even though all other events involved smaller volumes than the two manually identified ones. The initial filter frequency window for the STA-LTA-ratio approach of 10–30 Hz might have benefited from a lower cutoff frequency since some of the rockfalls showed optimal location frequencies well below this value (table 1).

The monitored section of the Lauterbrunnen Valley is a comparably noisy environment. The example PSD (fig. 4 a) shows ample signals from sources other than rockfall activity. A major source of falsely picked events was passing trains (87 %). For rockfalls as small as those detected in this study, raising the initial SNR threshold to exclude signals associated with train activity would result in rejecting most of the rockfall events. However, for rockfall volumes one or more orders of magnitude larger, this simple parameter adjustment should yield a significantly better detection result. The 19 detected earthquakes could have been removed based on differences in the relationships between magnitude, duration ~~or frequency content~~ and frequency content (e.g., Manconi et al., 2016) or multivariate classification approaches (e.g., Provost et al., 2017). However, the duration distributions of rockfalls versus earthquakes already allowed a sufficient discrimination. Thus, although the data processing work flow is far from automatic and leaves one order of magnitude more events than the actual number determined from manual evaluation, it provides a systematic and reproducible way to detect rockfalls close to the lower limit of detection.

6.2 Rockfall location

All ten TLS-based rockfall events were confirmed with an average location error along the rockfall trajectory of 33 m when the frequency window of the location algorithm was adjusted manually. Without this optimisation, which is only possible when reference data are available, the location deviation was 81 m on average. This is comparable with errors of about 80 m from a rock avalanche study on Montserrat, Lesser Antilles, ~~using a similar location approach~~ with a network of 11 stations (Levy et al., 2015). However, that study had a larger network aperture and focused on event volumes of 10^3–10^6 m^3. Instead, rock mass volumes in the Lauterbrunnen Valley were generally well below 1 m^3 and our study had only four operating seismic stations, organised in topology and station spacing comparable to those from other studies ~~(Lacroix and Helmstetter, 2011; **?**; Burtin et al., 2016)~~(Hibe

The TLS-based detachment locations and their rockfall trajectories are within the areas defined by the 0.95 quantile threshold (fig. 8). Only when independent constraints on the location of the seismically recorded events are available, is it possible to investigate the validity and effectiveness of this arbitrary threshold. In this study area, the threshold can be increased up to ~~0.9726~~ 0.973 to still provide a valid uncertainty estimate for possible rockfall locations/trajectories. Effectively, this means that the area of each uncertainty polygon can be decreased by 45 %.

An important issue is that for some rockfalls the best location estimate (P_{max}) is above the actual rockfall detachment zone. This may be related to the extreme topography of the Lauterbrunnen Valley. The studied rockwall is up to 800 m high, yet it is represented by as little as four plan view pixels in the 10 m DEM and distance maps (cf. ranges of z_{seis} in table 1). Arguably, the lateral offset of rockfall location P_{max} from the line of steepest descend is more important from a hazards point of view.

Assigning the locations of the ten seismically detected rockfalls to those detected by TLS is unambiguous in most cases. However, rockfalls with comparable volumes from similar detachment heights can be hard to distinguish. For example, events 3 and 4 are located 44 m apart, at 1108 and 1064 m asl., and released 0.201 and 0.175 m^3 of rock, respectively. Accordingly, their seismic waveforms and PSDs (fig. 8) look very similar and there remains ambiguity about the seismic identification as stated in table 1. This has consequences for the temporal information associated with the seismic data. But in this case, both events occurred on 20 October, one at 3 pm, the other at 7 pm. Ambiguity also arises for events 1 and 2. However, there the rockfall volumes allow for a better matching with the seismic results. Event 1 entrained 0.201 m^3 whereas event 2 ~~displaced~~

mobilised only 0.063 m^3 from a near identical position and fall height. Accordingly, the emitted seismic energy of event 1 should be significantly higher than event 2, which is reflected in the corresponding PSD, where event 1 shows a much longer and more powerful signal. Hence, if the geometric properties of the released rock masses are sufficiently distinct, it is possible to disentangle nearby events from the detailed seismic information.

For large ($> 10^4$ m^3) ~~rockslides and rock avalanches~~ gravitational mass wasting processes there appear to be robust relationships between released volumes and a series of seismic attributes ~~(?Ekström and Stark, 2013)~~(Dammeier et al., 2011; Ekström and Stark, 20 However, such large events affect significant areas, even entire slopes. In contrast, the small volumes mobilised in the Lauterbrunnen Valley do not show such ~~relationships~~clear volume-based relationships (apart from the one example described above). The largest event (2.338 m^3) did not yield the highest signal intensities or longest duration, and vice versa for the smaller events. The combination of released volume, detachment height above cliff base, the number, distance and strength of intermediate impacts, the degree of fragmentation during the fall phase and the fate to the rock mass on the talus slope (direct deposition, subsequent downhill translocation, entrainment of impacted talus) result in a polymorphic seismic signal, which complicates direct links of seismic parameters with geometric or kinetic properties of the detected rockfalls at this spatial scale. To explore such questions about relations among volume, detachment height, fragmentation and debris entrainment upon impact – all obviously more useful for larger rock volumes than found in this study – the combination of TLS and seismic monitoring provides all necessary sources of information. The high temporal resolution and ability to detect small volumes makes especially the seismic technique perticularly interesting for studies of relations between rockfalls and environmental conditions that are suspected to cause them (Dietze et al., 2017).

The apparent seismic detection limit for rockfall volumes in the Lauterbrunnen Valley is well below 1 m^3. This is remarkable given that the stations are mostly more than one km apart and that most of the rockfalls used for validation originated at the lower cliff parts, resulting in limited kinetic energy upon impact. Location feasibility is however not only determined by the rockfall volume and drop height. The distance between impact location and location of the seismic stations, the inelastic attenuation properties of the rock and the energy dissipation due to rock fragmentation ~~(e.g., ?)~~ (e.g., Hibert et al., 2011) also determine the potential to successfully locate the rockfall. The possibility to analyse rockfalls as small as 0.053 m^3, impacting at distances of 170–1950 m from the seismic stations, makes seismic monitoring a method that is able to reveal events well below the resolution of most other post-event survey techniques with the exception of TLS surveys.

Unlike other rockfall survey techniques, seismic methods allow for monitoring of rockfalls with high temporal resolution, down to fractions of a second. During the first half of the monitored month only two rock masses were released, while the other half of the month saw the majority of events. Beyond this, the high temporal resolution allows connecting the events to ambient conditions and trigger mechanisms, and to study process interactions ~~(cf. Burtin et al., 2014)~~(e.g., Helmstetter and Garambois, 2010; Burtin

6.3 Rockfall anatomies

Seismic monitoring allows detailed insight into the dynamics of rockfalls. The example event (fig. 2) consists of three distinct phases and lasts in total for almost a minute. Phase 1 (less than one s duration) is the first notable seismic activity after minutes of calm at all stations. It reflects the seismic signal associated with initiation of the rockfall event. The high frequency content ~~most likely corresponds to the~~ may either correspond to the rebound of the cliff after detachment of the mass (e.g., Hibert et al., 2011) or the opening and propagation of fractures rather than impacts of a moving rock mass. ~~This~~ The latter interpretation is supported by seismic records from the Illgraben, Rhone Valley, Switzerland, that show an exponentially increasing density of signals, which indicate cracking or fracture propagation (Zeckra et al., 2015) starting days before a 10^4 m^3 large rock avalanche took place (Burtin et al., 2016). The spectral properties of these signals (short, less than 1 s pulses at 20–50 Hz), recorded by a seismic station about 150 m away from the initiation zone of the rockslide are very similar to the first phase of the rockfall from the Lauterbrunnen Valley (fig. 2).

Phase 2 (one s duration) begins 1.7 s after this fracture propagation phase and may reflect the impact of the released rock mass on the cliff face. The predominantly low frequency content implies that the mass is still intact upon the first collision. Low frequencies can only be generated by large rock masses that convey a high momentum rather than a series of smaller particles hitting a surface simultaneously (Burtin et al., 2016). The strong impact likely caused fragmentation of the rock, because there is no low frequency content in any of the later signals from this event. The rock fragments experienced a free fall phase (calm period in all signal waveforms) of approximately 7.5 s, corresponding to a drop height of 271 m. With a detachment elevation between 1048–1123 m asl. this places the impact somewhere in the central part of the talus slope that reaches from 910 m asl. at the cliff base to 820 m asl. on the valley floor.

Phase 3 (about 40 s duration) represents the continuous impact of the fragmented rock mass on the talus slope for tens of seconds. This activity very likely graded into a phase of downslope translocation of debris and entrainment of further talus~~,~~ ~~because the~~. The PSD of phase 3 shows ~~a gradual shift from higher to lower frequencies with time. This is likely due to the longer lasting downslope transport of larger particles due to their higher momentum.~~

~~This~~ the typical properties characteristic for rock avalanches (e.g., Suriñach et al., 2005).

Similar insights to event anatomy is possible for the remaining nine events, though often with less rich detail or variability. Readers are invited to explore the data contained in the supplementary materials. This one anatomy of an example event highlights the universality of seismic sensors to investigate the dynamics of a rapid mass wasting process at a level of detail that would otherwise require an expensive and time-consuming multi-sensor approach, consisting of, for example, video imagery, prior and a posteriori TLS scans, perhaps further acoustic sensors, and post-event field mapping. Furthermore, the area of interest can only be small to be covered by these alternative techniques. Thus, the installation must be placed at “the right spot”, instead of relying on the flexibility to monitor a wider area with a seismic network.

7 Conclusions

The detachment locations of ten rockfall events, totalling a volume of 4.789 ± 0.100 m^3, were detected by TLS over 37 days. Using broadband seismometers, these events were independently detected and located with an average deviation of 81^{+59}_{-29} m. Further seismic rockfall signals were detected and located outside this instrumented cliff area. The seismic signatures allow i) insight into the dynamics of single events, ii) quantification of the exact event onset time and duration, and iii) calculating minimum fall heights. ~~Volume estimates based on the emitted seismic energy or peak ground acceleration were not possible for~~

~~the small rockfall events identified in this study. This was mainly due to the influence of intrinsic factors, such as the proportion of energy consumed for fragmentation during the event or contribution of mobilised debris to the seismic signals upon impact on the talus slope. However, the~~ The method allows detecting rockfalls with volumes as small as 0.053 m^3.

Results presented in this study suggest that seismic monitoring is a valid approach to holistic ~~detection, location and characterisation of~~ detecting, locating and characterising rockfall activity, also for comparably small events in terms of mobilised volumes and fall heights. The aperture of the seismic array (3 km) is comparable to other natural scale experiments ~~(e.g., Burtin et al., 2014; Lacroix and Helmstetter, 2011)~~ (e.g., Lacroix and Helmstetter, 2011; Burtin et al., 2014) and allows almost catchment-wide monitoring of Earth surface activity in an exceptionally steep terrain. Results from this study complement work that has focused on the coupling of rockfall to other processes in the sediment cascade of mountainous landscapes (e.g., Krautblatter et al., 2012).

The main limitations include that volume estimates based on the emitted seismic energy or peak ground acceleration were not possible for the small rockfall events identified in this study. This was mainly due to the influence of intrinsic factors, such as the proportion of energy consumed for fragmentation during the event or contribution of mobilised debris to the seismic signals upon impact on the talus slope. A further challenge is the high effort due to manual removal of false events under such conditions. This drawback represents a serious issue when attempting fully automated approaches of rockfall detection.

The combined description of event location and precise timing information of rockfall activity is a key step ~~to assess triggering mechanisms~~ towards assessing trigger mechanisms (Dietze et al., 2017). However, the number of events detected over the observation period of this study prohibits a statistical analysis of the ~~triggering~~ trigger mechanism for each event because the population size is too small. At larger scales (regarding released volumes and monitored area) there are first order effects that allow relating seismic metrics to process parameters ~~(e.g., ?Dammeier et al., 2011; Ekström and Stark, 2013)~~(e.g., Hibert et al., 2 Thus, when increasing the monitored area and focusing on larger released volumes ($> 10^4$ m^3), environmental seismology could become a real alternative to classic rockfall observatory instruments, with the capability to go beyond these by simultaneously recording proxies of environmental triggers and resolving process coupling and interaction.

It is possible to monitor rockfalls sensu ~~strictu~~ stricto with a significant free fall phase and a pronounced short impact phase. This extends the previous field of applications of environmental seismology to more extreme settings. Furthermore, seismic monitoring is not restricted to the instrumented cliff face but allows detection of rockfall signals from other areas such as the other valley wall and locations higher up in the catchment, though with sometimes only poor constraints on the location of these events.

There is ~~significant~~ potential to optimise the parameters for event location but there is no straightforward way to do this without independent auxiliary information. Hence, a realistic location error range along the trajectory of released rocks is 52–140 m (interquartile range). The height and location of the detachment zone can only be provided by seismic methods if the detachment process can be recorded and the subsequent impacts of the released rock mass can be located with sufficient confidence to allow back-calculation of the falling time. Rockfall release zones that are separated below the level of seismic location confidence can be deciphered from each other if the released volumes are different from each other and generate sufficiently distinct seismic characteristics. Hence, combining seismic and TLS methods can provide a very detailed complementary picture of rockfall activity.

8 Data and code availability

The seismic data used in this study is available in the supplementary materials, along with a detailed documentation about how to use it to reproduce the results of this study. The digital elevation model data set cannot be made freely available, but may be replaced by equivalent data to reproduce the results. TLS point cloud data are available upon request.

Author contributions. Michael Dietze contributed to seismic fieldwork and data analysis. Solmaz Mohadjer contributed to TLS fieldwork and data processing. Jens M. Turowski, Todd A. Ehlers and Niels Hovius contributed to equipment provision, project planning and data analysis. All authors contributed to manuscript preparation.

Acknowledgements. The field work campaigns generously benefited from the support of Maggi Fuchs, Michael Krautblatter, Torsten Queißer and Fritz Haubold. The authors are thankful for these creative involvements. We further thank Josy Burke and Lorenz Michel for TLS field assistance. We are also thankful to the GIPP seismic device pool for providing six TC120s sensors and Cube^3 data loggers.

References

Allen, R.: Automatic phase pickers: Their present use and future prospects, Bulletin of the Seismological Society of America, 72, S225–S242, 1982.

Bivand, R. S., Pebesma, E. J., and Gomez-Rubio, V.: Applied spatial data analysis with R, Springer, 2013.

Bourbie, T., Coussy, O., and Zinszner, B.: Acoustics of porous media, Gulf Publishing Company, 1987.

Burtin, A., Bollinger, L., Vergne, J., Cattin, R., and Nabelek, J. L.: Spectral analysis of seismic noise induced by rivers: A new tool to monitor spatiotemporal changes in stream hydrodynamics, Journal of Geophysical Research, 113, B05 301, doi:10.1029/2007JB005034, 2008.

Burtin, A., Bollinger, L., Cattin, R., Vergne, J., and Nabelek, J. L.: Spatiotemporal sequence of Himalayan debris flow from analysis of high-frequency seismic noise, Journal of Geophysical Research: Earth Surface, 114, n/a–n/a, doi:10.1029/2008JF001198, f04009, 2009.

Burtin, A., Hovius, N., Milodowski, D. T., Chen, Y.-G., Wu, Y.-M., Lin, C.-W., Chen, H., Emberson, R., and Leu, P.-L.: Continuous catchment-scale monitoring of geomorphic processes with a 2-D seismological array, Journal of Geophysical Research, 118, 1956–1974, doi:0.1002/jgrf.20137, 2013.

Burtin, A., Hovius, N., McArdell, B. W., Turowski, J. M., and Vergne, J.: Seismic constraints on dynamic links between geomorphic processes and routing of sediment in a steep mountain catchment, Earth Surface Dynamics, 2, 21–33, doi:10.5194/esurf-2-21-2014, 2014.

Burtin, A., Hovius, N., and Turowski, J. M.: Seismic monitoring of torrential and fluvial processes, Earth Surface Dynamics, 4, 285–307, doi:10.5194/esurf-4-285-2016, 2016.

Dammeier, F., Moore, J. R., Haslinger, F., and Loew, S.: Characterization of alpine rockslides using statistical analysis of seismic signals, Journal of Geophysical Research, 116, F04 024, doi:10.1029/2011JF002037, 2011.

Dietze, M.: eseis: Environmental seismology toolbox, r package version 0.3.1, 2016.

Dietze, M., Turowski, J. M., Cook, K. L., and Hovius, N.: Spatiotemporal patterns and triggers of seismically detected rockfalls, Earth Surface Dynamics Discussions, 2017, 1–33, doi:10.5194/esurf-2017-20, http://www.earth-surf-dynam-discuss.net/esurf-2017-20/, 2017.

Ekström, G. and Stark, C. P.: Simple Scaling of Catastrophic Landslide Dynamics, Science, 339, 1416–1419, doi:10.1126/science.1232887, 2013.

FOEN: Hydrological data and forecasts, Available at http://www.hydrodaten.admin.ch/en/2200.html (2017/04/11), 2017.

Gimbert, F., Tsai, V. C., and Lamb, M. P.: A physical model for seismic noise generation by turbulent flow in rivers, Journal of Geophysical Research, 119, 2209–2238, doi:10.1002/2014JF003201, 2014.

Havskov, J. and Alguacil, G.: Instrumentation in earthquake seismology, Modern Approaches in Geophysics 22, Springer, 2006.

Helmstetter, A. and Garambois, S.: Seismic monitoring of Sechilienne rockslide (French Alps): Analysis of seismic signals and their correlation with rainfalls, Journal of Geophysical Research, 115, F03 016, doi:10.1029/2009JF001532, 2010.

Hibert, C., Mangeney, A., Grandjean, G., and Shapiro, N. M.: Slope instabilities in Dolomieu crater, Réunion Island: From seismic signals to rockfall characteristics, Journal of Geophysical Research, 116, F04 032, doi:10.1029/2011JF002038, 2011.

Hibert, C., Mangeney, A., Grandjean, G., Baillard, C., Rivet, D., Shapiro, N. M., Satriano, C., Maggi, A., Boissier, P., Ferrazzini, V., and Crawford, W.: Automated identification, location, and volume estimation of rockfalls at Piton de la Fournaise volcano, Journal of Geophysical Research, 119, 1082–1105, doi:10.1002/2013JF002970, 2014.

Hijmans, R. J.: raster: Geographic Data Analysis and Modeling, https://CRAN.R-project.org/package=raster, r package version 2.5-8, 2016.

Krautblatter, M., Moser, M., Schrott, L., Wolf, J., and Morche, D.: Significance of rockfall magnitude and carbonate dissolution for rock slope erosion and geomorphic work on Alpine limestone cliffs (Reintal, German Alps), Geomorphology, 167-168, 21–34, doi:10.1016/j.geomorph.2012.04.007, 2012.

Lacroix, P. and Helmstetter, A.: Location of Seismic Signals Associated with Microearthquakes and Rockfalls on the Séchilienne Landslide, French Alps, Bulletin of the Seismological Society of America, 101, 341–353, doi:10.1785/0120100110, 2011.

Larose, E., Carrière, S., Voisin, C., Bottelin, P., Baillet, L., Guéguen, P., Walter, F., Jongmans, D., Guillier, B., Garambois, S., Gimbert, F., and Massey, C.: Environmental seismology: What can we learn on earth surface processes with ambient noise?, Journal of Applied Geophysics, 116, 62–74, doi:10.1016/j.jappgeo.2015.02.001, 2015.

Levy, C., Mangeney, A., Bonilla, F., Hibert, C., Calder, E. S., and Smith, P. J.: Friction weakening in granular flows deduced from seismic records at the Soufrière Hills Volcano, Montserrat, Journal of Geophysical Research: Solid Earth, 120, 7536–7557, doi:10.1002/2015JB012151, 2015.

Lin, C. H., Jan, J. C., Pu, H. C., Chen, C. C., and Wu, Y. M.: Landslide seismic magnitude, Earth and Planetary Science Letters, 429, 122–127, doi:10.1016/j.epsl.2015.07.068, 2015.

Manconi, A., Picozzi, M., Coviello, V., De Santis, F., and Elia, L.: Real-time detection, location, and characterization of rockslides using broadband regional seismic networks, Geophysical Research Letters, 43, 6960–6967, doi:10.1002/2016GL069572, 2016.

Pebesma, E. J. and Bivand, R. S.: Classes and methods for spatial data in R, R News, 5, 2005.

Pebesma, E. J. and Bivand, R. S.: sp: Classes and Methods for Spatial Data, https://CRAN.R-project.org/package=sp, r package version 1.2-3, 2016.

Provost, F., Hibert, C., and Malet, J.-P.: Automatic classification of endogenous landslide seismicity using the Random Forest supervised classifier, Geophysical Research Letters, 44, 113–120, doi:10.1002/2016GL070709, 2017.

R Development Core Team: R: A Language and Environment for Statistical Computing, Vienna, Austria, http://CRAN.R-project.org, 2015.

Rabatel, A., Deline, P., Jaillet, S., and Ravael, L.: Rock falls in high-alpine rock walls quantified by terrestrial lidar measurements: A case study in the Mont Blanc area, Geophysical Research Letters, 35, doi:10.1029/2008GL033424, 2008.

Ring, J.: The laser in astronomy, New Scientist, 344, 672–673, 1963.

Stock, G., Collins, B., Santaniello, D., Zimmer, V., Wieczorek, G., and Snyder, J.: Historical rock falls in Yosemite National Park, U.S. Geological Survey Data Series 746, 746, 17, 2013.

Strunden, J., Ehlers, T. A., Brehm, D., and Nettesheim, M.: Spatial and temporal variations in rockfall determined from TLS measurements in a deglaciated valley, Switzerland, Journal of Geophysical Research, 120, 1–23, doi:10.1002/2014JF003274, 2014.

Suriñach, E., Vilajosana, I., Khazaradze, G., Biescas, B., Furdada, G., and Vilaplana, J. M.: Seismic detection and characterization of landslides and other mass movements, Natural Hazards and Earth System Sciences, 5, 791–798, 2005.

Vilajosana, I., Surinach, E., Abellan, A., Khazaradze, G., Garcia, D., and Llosa, J.: Rockfall induced seismic signals: case study in Montserrat, Catalonia, Natural Hazards and Earth System Sciences, 8, 805–812, 2008.

Volkwein, A., Schellenberg, K., Labiouse, V., Agliardi, F., Berger, F., Bourrier, F., Dorren, L. K. A., Gerber, W., and Jaboyedoff, M.: Rockfall characterisation and structural protection – a review, Natural Hazards and Earth System Sciences, 11, 2617–2651, doi:10.5194/nhess-11-2617-2011, 2011.

Welch, P.: The use of fast Fourier transform for the estimation of power spectra: A method based on time averaging over short, modified periodograms, IEEE Transactions on Audio and Electroacoustics, 15, 70–73, 1967.

Zeckra, M., Hovius, N., Burtin, A., and Hammer, C.: Automated Detection and Classification of Rockfall Induced Seismic Signals with Hidden-Markov-Models, 2015 AGU Fall Meeting 2015 - NH34A-04, 2015.

Zimmer, V. L. and Sitar, N.: Detection and location of rock falls using seismic and infrasound sensors, Engineering Geology, 193, 49–60, 2015.

Zimmer, V. L., Collins, B. D., Stock, G. M., and Sitar, N.: Rock fall dynamics and deposition: an integrated analysis of the 2009 Ahwiyah Point rock fall, Yosemite National Park, USA, Earth Surface Processes and Landforms, 37, 680–691, doi:10.1002/esp.3206, 2012.